gineering
Library

JUL 22 '46

UNITED STATES DEPARTMENT OF COMMERCE

Journal of Research

of the

National Bureau of Standards

Vol. 36, No. 4 April 1946

CONTENTS

RP	TITLE AND AUTHOR	Page
1705.	Spectographic determination of boron in steel. Charles H. Corliss and Bourdon F. Scribner.....[Price 5 cents]	351
1706.	Hygroscopicity of optical glasses as an indicator of serviceability. Donald Hubbard.....[Price 5 cents]	365
1707.	Solubility of cadmium sulfate in H_2O-D_2O mixtures. Langhorne H. Brickwedde.....[Price 5 cents]	377
1708.	A glossmeter for smoothness comparisons of machine-finished surfaces. Richard S. Hunter.....[Price 5 cents]	385
1709.	Absorption and scattering by sound-absorbent cylinders. Richard K. Cook and Peter Chrzanowski.....[Price 10 cents]	393
1710.	Dynamic tensile tests of parachute webbing. Ambrose H. Stang, Martin Greenspan, and Sanford B. Newman...[Price 5 cents]	411
1711.	Note on the density and heat of combustion of benzoic acid. R. S. Jessup.....[Price 5 cents]	421

The articles listed may be purchased separately (see cover page II) at the prices stated

A monthly periodical of pure and applied science published by our National Government

Journal of Research
of the
National Bureau of Standards

The January 1946 issue of the JOURNAL OF RESEARCH of the National Bureau of Standards began the thirty-sixth semiannual volume of this periodical. Fundamental researches in progress in the Bureau's laboratories are reported in this JOURNAL. If you are interested in new developments in science and technology, you should receive the JOURNAL. If you are not already a subscriber, you are invited to send in your subscription.

Technical News Bulletin

This is a monthly publication containing short articles reporting progress of work in the Bureau laboratories, abstracts of papers that appear in the JOURNAL OF RESEARCH, accounts of scientific and technical meetings in which the Bureau has taken part, a list of all publications by members of the staff, and other items within the Bureau's fields. The BULLETIN is designed primarily to give a general and timely review of the activities of the Bureau in brief form. It is a prompt and reliable source of official information. If you have not already subscribed for the BULLETIN, you are invited to do so.

ANNUAL SUBSCRIPTION	Price	
	United States, Canada, Cuba, Mexico, Newfoundland, Republic of Panama	Other countries
JOURNAL OF RESEARCH of the National Bureau of Standards:		
12 monthly issues (2 volumes), paper covers	$3.50	$4.50
Bound volume (½ year, 1 volume), blue buckram	3.00	3.50
Technical News Bulletin, 12 monthly issues	.50	.70

Research Papers, reprinted individual articles appearing in the JOURNAL OF RESEARCH, are available from the Superintendent of Documents shortly after appearance of monthly issues of the JOURNAL.

Address orders only to
Superintendent of Documents, U. S. Government Printing Office
Washington 25, D. C.

UNITED STATES DEPARTMENT OF COMMERCE
HENRY A. WALLACE, Secretary
NATIONAL BUREAU OF STANDARDS
E. U. Condon, Director

✦

Journal of Research

of the

National Bureau of Standards

✦

Volume 36, Number 4

April 1946

[Published with approval of the Director of the Budget]

UNITED STATES
GOVERNMENT PRINTING OFFICE
WASHINGTON : 1946

For sale by the Superintendent of Documents, U. S. Government Printing Office
Washington 25, D. C. Price 30 cents, $3.50 per year on subscription

The prices of the separate Research Papers appearing in this JOURNAL are given on the front cover page. If 100 or more copies of any separate are ordered, a discount of 25 percent is allowed. Those who desire copies of separate Research Papers should send their orders and remittances without delay to the Superintendent of Documents, U. S. Government Printing Office, Washington 25, D. C. Research Papers are not printed from electrotypes, and usually no more reprints can be had when the first and only printing is exhausted.

MATHEMATICAL TABLES

A list of the mathematical tables now obtainable from the National Bureau of Standards is printed on pages 3 and 4 of the JOURNAL cover. New tables will be announced from time to time as they become available. An order blank is available on the last page of this issue.

U. S. Department of Commerce National Bureau of Standards

RESEARCH PAPER RP1705

Part of Journal of Research of the National Bureau of Standards, Volume 36, April 1946

SPECTROGRAPHIC DETERMINATION OF BORON IN STEEL [1]

By Charles H. Corliss and Bourdon F. Scribner

ABSTRACT

The spectrographic determination of small amounts of boron in thin steel rods and in massive pieces of steel was investigated by using several types of arc-like discharges. The sensitivity and accuracy in determining boron were found to be affected by variations in the rate of cooling of the electrodes. With 3/32-inch-rod electrodes, the high-voltage alternating-current arc permits determinations down to 0.0006 percent of boron, with an average deviation of ±4 percent. With more massive specimens the high-voltage alternating-current arc is insensitive, but an overdamped condenser discharge or similar source provides adequate sensitivity and precision. Determinations as low as 0.0001 percent of boron are made with a direct-current arc to which sodium is added to suppress an interfering Fe II line. In the course of the investigation, a series of six boron steels in two sizes, 3/32- and 1/2-inch rods, were issued as National Bureau of Standards Standard Samples covering the range 0.0006 to 0.019 percent of boron.

CONTENTS

	Page
I. Introduction	351
II. Determination of boron	352
1. General aspects of the problem	352
2. Determination of boron in thin-rod samples	353
3. Determination of boron in massive samples	357
(a) Overdamped condenser discharge	357
(b) Direct-current arc of low excitation energy	361
III. Spectrographic boron-steel standards	362
IV. References	364

I. INTRODUCTION

The addition of a few thousandths percent of boron to certain steels results in an increase in the hardenability (depth of hardening). This property suggested the possibility that boron could be substituted for considerably larger portions of strategic alloying elements in steel and, consequently, intensive studies of boron steels were made during the war period. Boron is commonly added to steel in the ladle or ingot molds in the form of ferroboron or by other addition agents containing various beneficial elements. In view of the low concentration of boron required for optimum hardening, usually 0.001 to 0.003 percent, and the effect of variations in concentration, accurate and rapid methods were required for its determination. This problem was brought to the Bureau's attention in connection with an investigation of the properties of boron steels by the Metallurgy

[1] Presented at the meeting of the Optical Society of America on October 19, 1945.

Division of this Bureau, the investigation being sponsored by the War Metallurgy Committee of the National Research Council, National Academy of Sciences. At the request of these groups, and with funds alloted by the Office of Production Research and Development of the War Production Board, methods were developed for the spectrographic determination of boron in solid steel specimens and, in addition, standard samples were made available for the use of other laboratories. A concurrent investigation of the chemical determination of boron by the Chemistry Division of this Bureau permitted intercomparison of methods and provided the chemical determinations essential to the certification of standards. The methods were applied in the analysis of armor plate and of other samples involved in metallurgical investigations.

Methods for the spectrographic determination of boron in various materials have been reported in the literature. For application to steels, Masi [1] [2] described a method employing solutions with spark excitation for determinations in the range 0.03 to 2.0 percent of boron. Schliessmann [2] investigated the sensitivity of detection of a number of components of steels, including boron, using solutions and arc excitation. His results indicated a sensitivity of 0.005 percent for boron. Recently, Gegechkori and Fal'kova [3] described a spark method similar to that of Masi for determinations of boron in the range of 0.1 to 1.0 percent and also an a-c arc method employing filings of the steel sample for the range 0.001 to 0.1 percent of boron. None of these methods employed the steel sample in solid form and all required time-consuming preliminary preparations. Irish [4] has recently described the application of the a-c arc method to the rapid determination of boron in the range 0.002 to 0.05 percent of boron, using rod samples. This method is quite satisfactory for control analysis where samples may be cast in reproducible shape, such as rods $\frac{7}{32}$ inch in diameter. However, the method must be employed under closely specified conditions, and its sensitivity falls off markedly if the size of the sample is increased. The methods to be described are applicable to rod or massive specimens in control testing and in the testing of fabricated parts. The requirement for the methods, that standard samples be available in suitable form, was met by the certification of six National Bureau of Standards Standard-Sample rods $\frac{7}{32}$ inch in diameter and a corresponding set of six standards, $\frac{1}{2}$ inch in diameter, each set covering the range 0.0006 to 0.019 percent of boron.

II. DETERMINATION OF BORON

1. GENERAL ASPECTS OF THE PROBLEM

The concentrations of boron commonly encountered in steels produced in this country are near the limit of spectrographic detection by the usual methods of excitation. As spark excitation is useful only for amounts of boron above 0.005 percent, arc excitation is employed under conditions adjusted to obtain maximum sensitivity. In order to extend the range of determination to 0.001 percent of boron or less, the limiting factors of interference by spectral background and by neighboring iron lines must be minimized. The unfortunate inter-

[1] Figures in brackets indicate the literature references at the end of this paper.

erence of the iron line Fe II 2497.82 A with the strongest boron line
I 2497.73 A renders the latter line unsuitable for analytical purposes
nder many observing conditions, and the next strongest boron line,
I 2496.78 A, is therefore employed. If the resolving power available
the spectrograph is sufficient to separate the first two lines, an
crease in sensitivity up to a factor of two would be realized by use
f the strongest boron line. Another possibility is the reduction of
tensity of the interfering Fe II line with respect to the strongest
I line. Because of the higher energy required for excitation of the
e II line as compared to the B I line, the former may be suppressed
y employing an excitation source of low energy. Advantage is
aken of this phenomenon, when the highest sensitivity is desired, by
mploying a d-c arc to which sodium is added to maintain low-level
xcitation.

Another factor of considerable importance in the determination
f boron is its volatility (probably as oxide), which is appreciably
igher than that of iron; this characteristic is both helpful and
roublesome. It permits enrichment of the vapor by boron under cer-
ain excitation conditions, thus increasing the sensitivity of detection.
A disadvantage lies in the care required to ensure reproducible heating
f the electrodes to obtain accurate determinations. Variations in
eat conduction from the discharge points on the electrodes may lead
o appreciable errors in the analytical results. Because of the
ffects of heat conduction, it was found necessary for optimum results
o apply different excitation procedures in determining boron in thin
ods and in more massive pieces.

The existence of boron in complexes insoluble in acids was observed
n the determination of boron by chemical analysis. As much as one-
alf of the boron may remain in the minute acid-insoluble residue
hen the total concentration of boron lies in the range of a few thou-
andths percent or less. The procedure for chemical analysis, there-
ore, provides for alkaline fusion of the insoluble material to incorporate
t in the solution. This time-consuming operation would necessarily
e involved in a solution method for spectrographic analysis and
consequently renders this procedure impracticable in comparison with
method of direct excitation of the steel sample. The existence of
oron in acid-soluble and acid-insoluble forms presents the possibility
hat these forms may differ in volatility in spectral excitation and may
ffect the spectrographic determinations. However, a comparison of
hemical and spectrographic results for samples having different
ractions of insoluble boron has not disclosed an appreciable effect
n the spectrographic results.

2. DETERMINATION OF BORON IN THIN-ROD SAMPLES

The determination of boron in thin-rod samples, for example, rods
$\frac{1}{32}$ inch (5.6 mm) in diameter, may be accomplished with satisfactory
ensitivity and accuracy by means of the usual arrangement of a
2,500-volt 10-kw a-c arc.[3] Under the conditions employed here for
he line B I 2496.78 A, the method exhibits a sensitivity of 0.0006
ercent of boron, with an average deviation of ±4 percent of the

[3] A 4-ampere d-c arc was found sensitive to 0.001 percent of boron with light from the entire arc stream or to 0.0006 percent of boron with light taken from a portion of the arc stream nearest the positive electrode. Determinations by this procedure, however, are not as precise as those obtained with the a-c arc.

amount present. The conditions employed in the a-c arc method a as follows:

Electrodes.—The tips of two rods ⅛ inch (5.6 mm) in diameter a ground to a 150-degree cone (the cone angle should be standardize throughout the procedure, but the value selected is not critical).

Mounting of electrodes.—The two rods are mounted in clip holde with each electrode protruding a fixed distance of 12 mm or more fro the holders to minimize heat conduction. The analytical gap is s at 1.8 mm.

Excitation.—A 2,500-volt a-c arc with current of 4.5 amperes is use

Spectrography.—A large Littrow quartz spectrograph with a sl width of 20 microns is employed with an Eastman Spectrum Analys No. 1 plate.

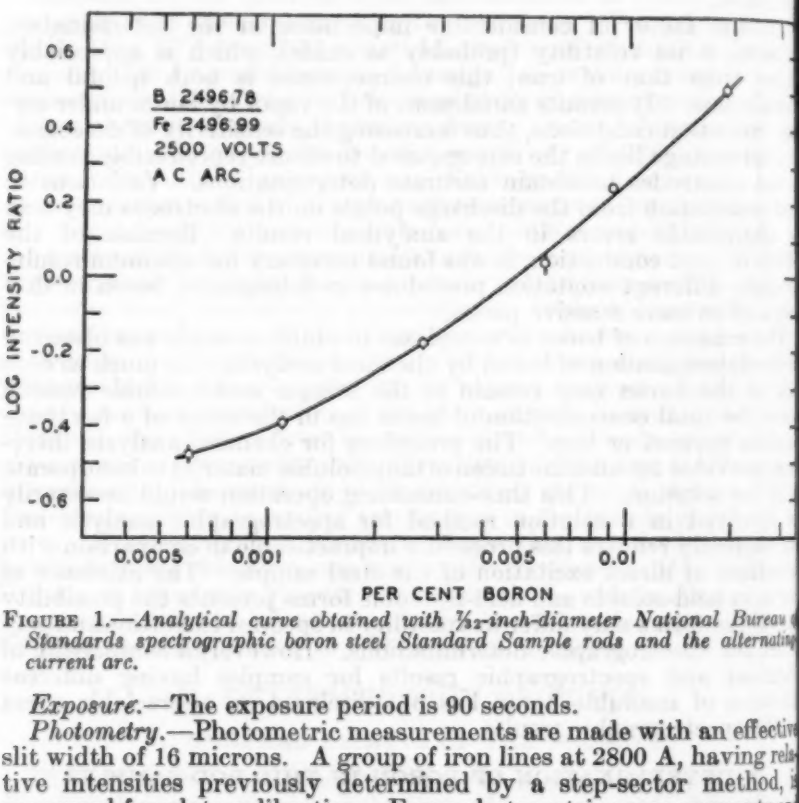

FIGURE 1.—*Analytical curve obtained with ⅛-inch-diameter National Bureau Standards spectrographic boron steel Standard Sample rods and the alternati current arc.*

Exposure.—The exposure period is 90 seconds.

Photometry.—Photometric measurements are made with an effecti slit width of 16 microns. A group of iron lines at 2800 A, having rel tive intensities previously determined by a step-sector method, measured for plate calibration. From photometric measurements an the calibration curve, the intensity ratio of B I 2496.78 A an Fe I 2496.99 A is obtained.

The analytical curve shown in figure 1 was constructed from th mean values of four determinations on each of the six National Bureau of Standards boron-steel Standard Samples Nos. 425 to 430, inclusive The spread of the runs for each standard is indicated by the length o the vertical line at each point; the mean of a set of values is given b the small circle. In order to accommodate the full range of concen

trations to the latitude of the plate, it was found necessary to reduce the intensity of the boron line above 0.006 percent by means of a step sector or filter. Determinations usually fall below this concentration in routine analysis. The precision of the method is demonstrated in table 1 by the results of repeated runs on the same sample.

TABLE 1.—*Precision of 2,500-volt a-c arc method*

[Seventeen runs of NBS Standard Sample 427 on one plate.]

Boron content	Deviation	Boron content	Deviation
Percent	*Percent*	*Percent*	*Percent*
0.00282	0.00012	0.00262	0.00008
.00256	.00014	.00288	.00018
.00271	.00001	.00286	.00016
.00261	.00009	.00269	.00001
.00270	.00000	.00266	.00004
.00281	.00011	.00253	.00017
.00277	.00007	.00258	.00012
.00278	.00008	.00262	.00008
.00275	.00005		
		[1] 0.00270	[1] 0.00009
Average deviation from the mean, ±4%			

[1] Average.

The accuracy of the results is difficult to estimate. The agreement of the plotted points with the smooth curve in figure 1 indicates an accuracy approaching the precision of the spectrographic results in these cases where carefully determined chemical values are available for comparison. In routine analyses, a comparison of spectrographic determinations (average of three runs) and single runs by chemical analysis showed an average deviation of $\pm 0.0003_6$ percent, or ± 19 percent of the amount present.

The sensitivity of detection of boron in steel with the a-c arc source depends on the temperature of the molten pool from which the steel is being vaporized into the arc stream. As the temperature is raised, the ratio of boron to iron vapor in the arc steam is increased. The temperature in turn depends on the rate of cooling of the rods and is markedly affected by the method of supporting the electrodes and by their diameter. This can be demonstrated by supporting two $\frac{7}{32}$-inch rods in closely fitting water-cooled copper clamps. The temperature of their tips will depend on the length of rod projecting from the clamps. In figure 2 the intensity ratio of boron to iron is plotted as a function of the distance to which the tips of the rods projected from the clamps. The marked effect of the variation of electrode temperature is apparent in the figure. At projections greater than 14 mm the temperature of the tips was unaffected by variations in the distance of projection as most of the cooling was by radiation and conduction into the air rather than by conduction through the rods into the clamps. This figure illustrates the importance of a proper method of supporting the electrodes and its possible effect on the sensitivity and the accuracy of the determinations.

Figure 3 shows another aspect of the same effect. Here the temperature of the tips of the rods decreased as the rod diameter was increased. As in figure 1, the intensity ratio of boron to iron is great-

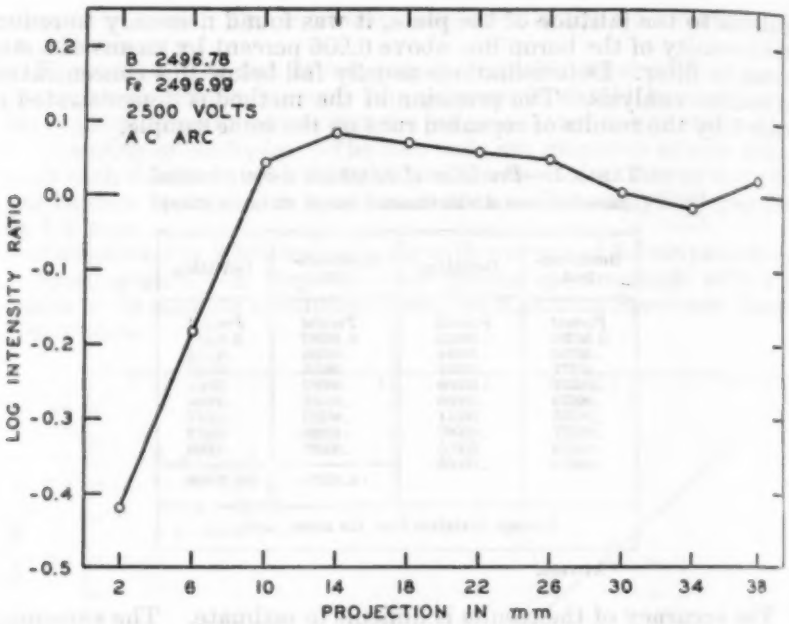

FIGURE 2.—*Effect of variation in projection of 1/32-inch-diameter rods from water-cooled copper clamps on the intensity ratio of boron to iron lines in the alternating-current arc.*

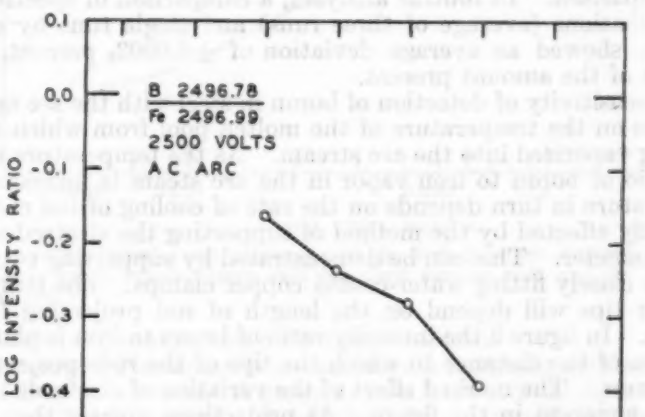

FIGURE 3.—*Effect of variation of rod diameter on the intensity ratio of boron to iron lines in the alternating-current arc.*

est where the temperature is highest. For this reason the ordinary 10-kw a-c arc provides inadequate sensitivity for determinations of boron on large samples, such as rods ½ inch in diameter or heavy fabricated pieces.

3. DETERMINATION OF BORON IN MASSIVE SAMPLES

If the steel samples are in the form of irregular massive pieces, it is advantageous to have a method for the determination of boron that does not require machining the steel to thin rods having a closely controlled diameter. The high-voltage a-c arc provides a sensitivity of only 0.005 percent with the boron line 2496.78 A when applied to massive pieces of steel, and therefore other modes of excitation were investigated. Three sources were found useful, namely, an overdamped condenser discharge, a high-current a-c arc, and a high-current d-c arc of low excitation energy. The procedures to be described for these excitation sources are applied with the point-to-plane electrode technic, in which one electrode is the steel sample having a machined flat surface at least ½ inch in diameter and the other electrode is a graphite rod.

(a) OVERDAMPED CONDENSER DISCHARGE

A commercial source of excitation, the Multisource unit, providing a wide selection of discharge conditions has been described by Hasler [5]. One mode of excitation involving the discharge of a condenser bank through relatively high values of inductance and resistance results in an overdamped discharge with favorable characteristics for the determination of boron. The method exhibits a sensitivity of 0.0006 percent of boron, with an average deviation of ±5 percent of the amount present and thus, with irregularly shaped steel specimens, matches the results obtained by the high-voltage a-c arc as applied to thin-rod samples. The conditions employed are as follows:

Electrodes.—A flat surface having a diameter of ½ inch (13 mm) or more is machined on the steel specimen. A counter electrode is prepared from ¼-inch (6.3 mm) boron-free graphite by cutting a 120-degree cone on the end.

Mounting of electrodes.—The steel electrode (positive) is mounted with its flat surface in a horizontal plane; the counter electrode (negative) is mounted vertically with an electrode gap of 6 mm. The half of the electrode gap above the steel electrode is centered on the optical path, and the image of this portion of the discharge is projected to the collimator lens of the spectrograph by means of a lens (*f*-34 cm) at the slit of the spectrograph.

Excitation.—An overdamped condenser discharge of the Multisource unit is employed with capacitance of 60 μf, inductance 480 μh, resistance 50 ohms, charging voltage 940 volts, and full initiator power.

Spectrography.—A large Littrow quartz spectrograph with a slit width of 20 microns is employed with an Eastman Spectrum Analysis No. 1 plate.

Exposure.—The exposure period is 90 seconds.

Photometry.—Photometric measurements are made as described for the a-c arc method, except that Fe I 2487.37 A is employed.

887131—46——2

The analytical curve shown in figure 4 was constructed from the mean values of three determinations on each of the six National Bureau of Standards Standard Samples 825 to 830, inclusive, having a diameter of ½ inch. The agreement of the points with the smooth curve indicates an accuracy approaching the precision of the spectrographic determinations. The precision of the method is demonstrated in table 2 by the results of repeated runs on Standard Sample 826.

Comparison of routine spectrographic determinations (average of three runs) and chemical determinations, by single runs, for boron in 24 steel samples showed an average deviation of 0.0003$_8$ percent, or ±17 percent of the amount present.

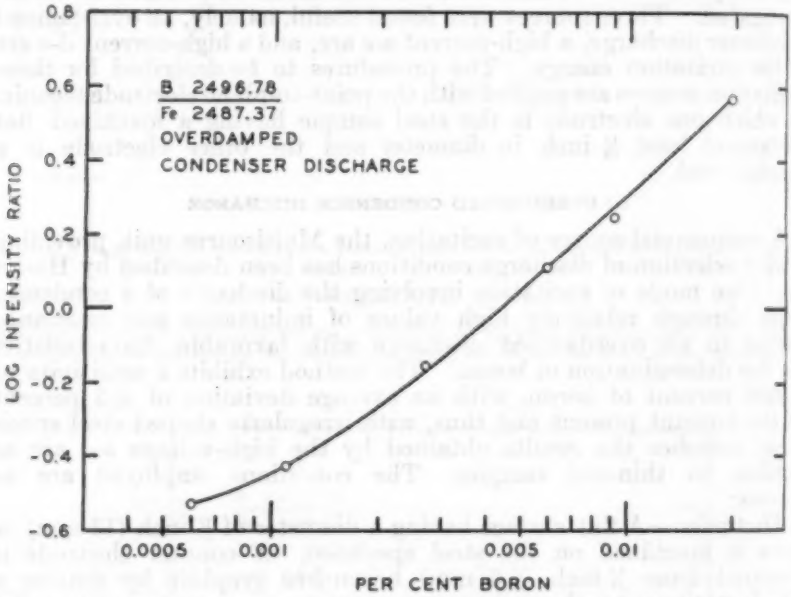

FIGURE 4.—*Analytical curve obtained with ½-inch-diameter National Bureau of Standards spectrographic boron steel Standard Samples and the overdamped condenser discharge.*

TABLE 2.—*Precision of overdamped condenser discharge*

[Sixteen runs of Standard Sample 826 on one plate]

Boron content	Deviation	Boron content	Deviation
Percent	*Percent*	*Percent*	*Percent*
0.00105	0.00005	.00103	.00007
.00110	.00006	.00125	.00015
.00117	.00007	.00106	.00004
.00099	.00011	.00108	.00002
.00115	.00005	.00113	.00003
.00109	.00001		
.00109	.00001	[1] .00110	[1] .00006
.00115	.00005		
.00098	.00012	Average deviation from the mean ±5 percent.	
.00114	.00004		
.00108	.00002		

[1] Average.

The operating conditions for the excitation source were selected to provide optimum sensitivity and reproducibility. The maximum value of capacity is necessary to provide sufficient intensity of the boron line. The effect of resistance in the circuit, as plotted in figure 5, shows that the intensity ratio of boron to iron reaches a maximum at 15 ohms but that the ratio of boron to background reaches a maximum at 20 ohms and remains nearly constant above that value. In view of the gain in the intensity of the boron line at higher resistance values,

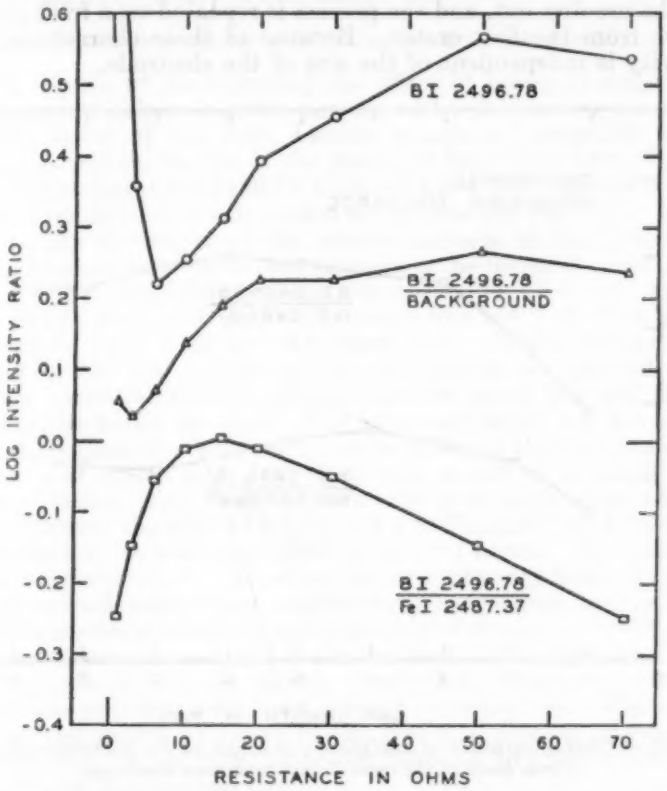

FIGURE 5.—*Effect of variation of resistance on the intensity ratio of boron to iron lines in the overdamped condenser discharge.*

a resistance of 50 ohms was adopted. Under these conditions the available variation in inductance has little effect on the discharge, but as larger inductance increased the intensity level slightly, the maximum value of 480 μh was employed. The intensity level also depends on the distance between the electrodes, as shown in figure 6. At larger gap distances the intensity ratio of boron to iron is little affected by change in the gap; the optimum gap distance apparently lies between 4 and 6 mm. The electrode polarity in which the steel electrode is positive provides maximum sensitivity; reversal of polarity reduces the intensity ratio of boron to iron by a factor of 4.5.

The high sensitivity of this discharge apparently results from a combination of a violent attack on the surface of the steel and a subsequent overdamped condenser discharge with a duration sufficient to volatilize and excite the metal under arc-like conditions. As each pulse of current passes between the electrodes, a molten pool of steel about ½ mm in diameter is formed and is explosively volatilized, ejecting droplets and leaving a minute crater on the steel surface. The boron volatilizes from the surface of the molten metal before heat conduction into the body of the steel electrode is well established. Then the arc dies out, and the process is repeated on a fresh spot at a distance from the first crater. Because of these characteristics the sensitivity is independent of the size of the electrode.

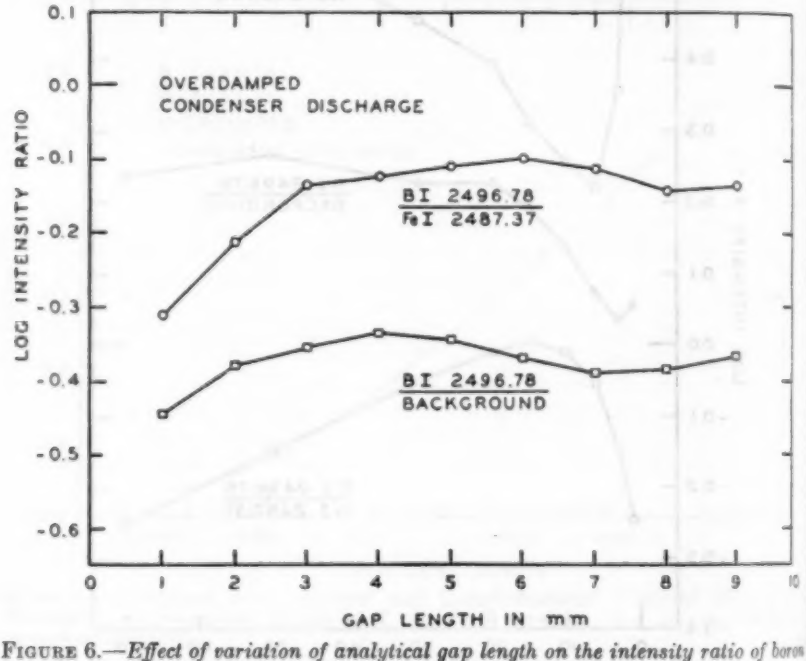

FIGURE 6.—*Effect of variation of analytical gap length on the intensity ratio of boron to iron lines in the overdamped condenser discharge.*

A series of determinations of boron made on steel specimens of different sizes and shapes but from the same heat of metal showed close agreement. If the sample provides a flat surface ½ inch in diameter or larger and is sufficiently massive to prevent excessive heating, an accurate determination can be made.

The possibility that the National Bureau of Standards boron-steel standards could be employed for the determination of boron in cast iron was investigated by use of this excitation method. A comparison of spectrographic and chemical results on three cast-iron samples showed the former to be low by 30 percent, indicating that cast-iron standards must be used.

If the Multisource unit is not available, a low-voltage a-c arc may be employed with comparable accuracy but with sensitivity limited to

0.001 percent of boron. This source offers the advantage, over the usual high-voltage a-c arc, in that larger currents may be passed through the arc, and consequently the selective volatilization of boron from massive specimens may be increased with a gain in sensitivity. The 220-volt a-c arc is not self-sustaining, but an auxiliary circuit similar to that described by Brockman and Hochgesang [6] provides a weak spark for steady ignition of the arc. The arc is run at a current of 7.5 amperes from a 220-volt a-c line with an electrode gap of 3 mm and an exposure of 30 seconds.

(b) DIRECT-CURRENT ARC OF LOW EXCITATION ENERGY

In the course of investigating the effect of boron in armor plate, determinations as low as 0.0001 percent of boron were required. The resolving power of the large Littrow quartz spectrograph was not sufficient to permit the use of the strongest boron line 2497.73 A, and the second strongest line 2496.78 A did not allow detection below 0.0006 percent of boron with the excitation procedures just described. As was stated in the discussion of the general aspects of the problem, an excitation means was found that permitted the use of B I 2497.73 A by minimizing the interference of the iron spark line Fe II 2497.82 A.

The energy needed to excite the boron line is 4.9 electron volts as compared to 16.1 volts for the spark line. If the energy of the electrons in the arc is reduced by introducing an element of low ionization potential, the intensity of the iron spark line will fall with respect to the boron arc line. This idea was tested in a d-c arc with the point-to-plane electrode combination in which the graphite counter electrode was drilled and then filled with a salt of an alkali metal. Of the elements tried, only sodium and potassium were effective. Sodium changed the ratio of B I 2497.73 A to Fe II 2497.82 A from unity at 0.003 percent to unity at 0.0003 percent of boron. Potassium was even more effective but reduced the general intensity level excessively. Not all sodium salts were satisfactory; anhydrous sodium sulfite provided superior sensitivity and precision of results.

For maximum accuracy with this method, the temperature of the steel electrode should be closely controlled. Large specimens of identical size and shape are least subject to variations. The physical form and concentration range of the National Bureau of Standards spectrographic boron steel Standard Samples are not suitable for application to this method.

The following conditions are employed:

Electrodes.—The anode is a steel block cut 1½ inches (38 mm) square by ½ inch (13 mm) thick and machined flat on both sides. The cathode consists of a ⅛-inch (3.2 mm) pure-graphite rod 15 mm long having a cup 2 by 2 mm filled with dry, powdered sodium sulfite.

Mounting of electrodes.—The steel block anode is mounted horizontally as the upper electrode. The cathode is inserted into a hole 5 mm deep in a ¼-inch graphite rod that serves as a mounting of low heat conductivity. The electrode gap is set at 6 mm, and light from a section of the gap 4 mm long at the steel electrode is focused on the collimator of the spectrograph.

Excitation.—A d-c arc is employed with current of 10 amperes drawn from a 220-volt line.

Spectrography.—The spectrum is photographed on a large Littrow quartz spectrograph with a slit width of 20 microns and using an Eastman No. 33 plate.

Exposure.—The exposure period is 90 seconds.

Photometry.—The plate is calibrated as described for the a-c arc method, and the intensity ratio of B I 2497.73 A to Fe I 2496.99 A is determined.

The analytical curve shown in figure 7 was constructed by this method from the mean values of three determinations on a set of five reference samples in which boron had been determined chemically. The agreement of repeated runs, as indicated by the vertical lines through the plotted points, is poor in comparison with the

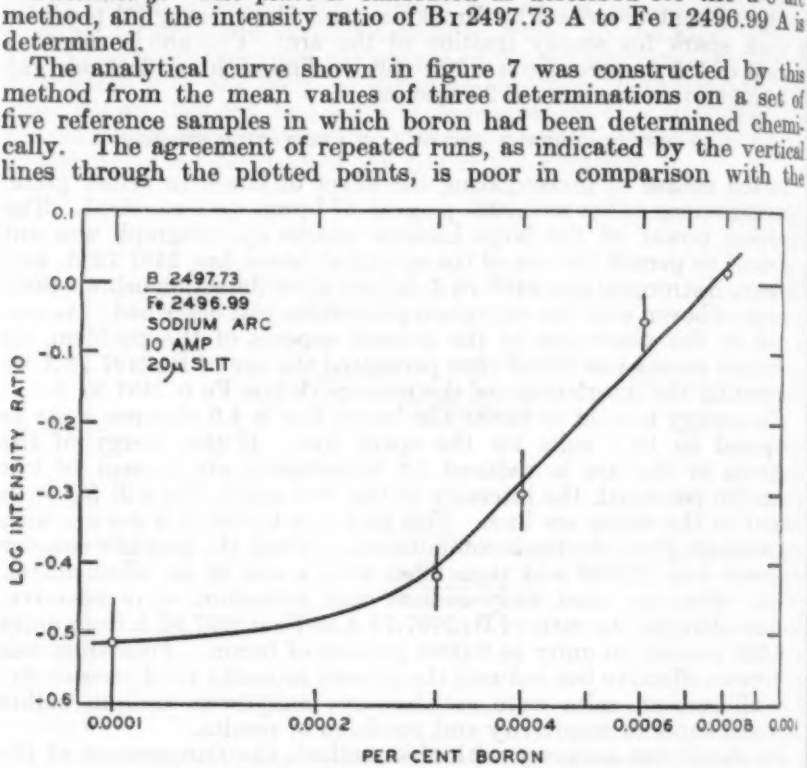

FIGURE 7.—*Analytical curve obtained for the determination of boron in steel with the sodium arc.*

methods just described. However, the mean of two determinations for an analytical sample provided results good to 0.0001 percent in most cases. The method is mainly useful for its high sensitivity and is not recommended for determinations above 0.001 percent of boron.

III. SPECTROGRAPHIC BORON-STEEL STANDARDS

The application of spectrographic methods involving direct excitation of the metallic sample requires standard samples, in proper forms, with uniform distribution of the element to be determined, and with accurate evaluation of its concentration. As a part of the investigation of methods for determining boron in steel, a series of boron steels was made available as National Bureau of Standards Standard Samples. The steels were obtained through the generous cooperation of the Bethlehem Steel Co., Bethlehem, Pa. For each standard, the steel of selected composition was hot-rolled to ⅛-and

$\frac{9}{32}$-inch rods, the rods were annealed, straightened, and finally finished to $\frac{1}{2}$ and $\frac{7}{32}$ inches, respectively, by centerless grinding. The finished rods, with the exception of Standard Sample 828 and part of 826, are in the annealed state.

The rods were received in 10-foot lengths at this Bureau, where a test sample was taken from both ends of each length. The samples were examined spectrographically, and the boron was found to be uniform within the precision of the spectrographic methods. The uniformity of compositions was gratifying, particularly as the boron was added in the furnace only in two cases, the remaining additions being made in the ladle or ingot molds. The boron contents of the standards were determined in the Chemistry Division of this Bureau by K. D. Fleischer. Boron in the 12 standards was determined by a distillation-tumeric colorimetric method and also by a distillation-titration method in the case of standards 427, 429, 430, 827, 829, and 830. The certified Standard Samples[4] and the modes of preparation are described in table 3.

TABLE 3.—*Spectrographic boron-steel Standard Samples*

Standard Sample number [1]	Type of steel	Addition agent	Added in—	Total boron
				Percent
425, 825	Mn-Ni-Cr B. O. H. (NE9450)	Ferroboron (11% boron)	Ingot	0.0006
426, 826	Cr-Mo B. O. H. (SAE 4150)	Grainal No. 79 (0.5% boron)	Ladle	.0011
427, 827	do	Ferroboron (12% boron)	do	.0027
428, 828	Mn-Cr B. O. H.	Ferroboron (11% boron)	do	.0059
429, 829	Ni-Cr-B (basic electric)	do	Furnace	.0091
430, 830	do	do	do	.019

[1] Standard Samples in the 400 series are rods $\frac{9}{32}$ inch in diameter, 4 inches long, and those in the 800 series are rods $\frac{1}{2}$ inch in diameter, 2 inches long.

The $\frac{7}{32}$-inch Standard Samples are intended for use as self-electrodes in the analysis of rods prepared in similar shape, for example, by the method described in section II–2. The 4-inch length may be cut at the center, yielding two rods, each 2 inches long. The larger standard rod provides a cross-sectional surface $\frac{1}{2}$ inch in diameter for application in the analysis of steel specimens of similar or larger size. If the Standard Samples are to be used with a Petry stand or a similar flat-top stand, it is convenient to mount them in a steel-disk adaptor fitted with six holes and setscrews for clamping the $\frac{1}{2}$-inch rods. Cutting the rods lengthwise to bridge the opening in the stand is not recommended. The $\frac{1}{2}$-inch standard rods also serve for the preparation of specimens of unusual shapes, such as square rods, and as a source of millings or turnings if these are desired.

The validity of applying the $\frac{1}{2}$-inch standards to the analysis of more massive specimens has been established by comparing the results on specimens having a variety of sizes but from the same heat of steel. If the specimen provides a flat surface $\frac{1}{2}$ inch in diameter or larger and has sufficient mass to avoid excessive heating, the Multisource unit and low-voltage a-c arc methods will apply accurately. Application of the usual d-c arc or of the sodium-arc procedure require samples and standards of identical size and shape.

[4] Full information on current National Bureau of Standards Standard Samples, including the procedure to be followed in their purchase, is given in the Supplement to NBS Circular C398, which can be obtained free upon application to the National Bureau of Standards, Washington 25, D. C.

IV. REFERENCES

[1] O. Masi, The spectrographic determination of boron in steels, Spectrochim. Acta **1,** 462–470 (1940).
[2] O. Schliessmann, The sensitivity of spectral analysis of alloy components of steel and iron, Arch. Eisenhüttenw. **15,** 167–174 (1941).
[3] N. M. Gegechkori and O. B. Fal'kova, Spectroanalytical determination of boron in steel, Zavodskaya Lab. **11,** 71–74 (1945).
[4] P. R. Irish, The application of spectrochemical analysis in the steel mill, J. Opt. Soc. Am. **35,** 226–233 (1945).
[5] M. F. Hasler and H. W. Dietert, A new spectroscopic source unit, J. Opt. Soc. Am. **33,** 218–228 (1943).
[6] F. G. Brockman and F. P. Hochgesang, Electrical ignition of the spectrographic arc, Ind. Eng. Chem., Anal. Ed. **14,** 796 (1942).

WASHINGTON, January 7, 1946.

U. S. DEPARTMENT OF COMMERCE NATIONAL BUREAU OF STANDARDS

RESEARCH PAPER RP1706

Part of Journal of Research of the National Bureau of Standards, Volume 36, April 1946

HYGROSCOPICITY OF OPTICAL GLASSES AS AN INDICATOR OF SERVICEABILITY

By Donald Hubbard

ABSTRACT

Several modifications of a powder-hygroscopicity method have been tried as a rapid means of determining the serviceability of optical glasses, i. e., their ability to maintain a clear polished surface under normal conditions of service. The method has been applied to a wide variety of glasses, and it shows the typical optical glasses in common use to be much less hygroscopic than the average commercial sheet and container glasses. In fact, many of the optical glasses even compare favorably with the better chemical laboratory wares, such as Pyrex, Tamworth, and Kimble N–51–a. This grouping of these glasses of such very dissimilar chemical durabilities serves well to emphasize that the capacity of a glass to maintain a clear surface upon exposure to the atmosphere, and its chemical durability as conventionally determined are two inherently different properties. A comparison of the hygroscopicity values of the Corning 015 electrode glass with those of the optical and chemical ware glasses whose electrode capacity is very poor suggests strongly that the pH response of a glass is primarily a function of its hygroscopicity. Tests made on a limited number of glasses of the binary series Na_2O-SiO_2, K_2O-SiO_2, Li_2O-SiO_2, and PbO-B_2O_3 appear to reflect some of the critical compositions of the respective phase equilibrium diagrams.

CONTENTS

	Page
I. Introduction	365
II. Experimental procedure	366
III. Results and discussion	367
1. Glasses of four binary systems	367
(a) Na_2O-SiO_2, K_2O-SiO_2, Li_2O-SiO_2	367
(b) PbO-B_2O_3 glasses	370
2. Comparison of some typical optical and other commercial glasses	371
IV. Conclusions	373
V. References	374

I. INTRODUCTION

The serviceability of optical glasses, namely, the ability to maintain a clear polished surface under normal service conditions, is too often confused with the general subject of the "chemical durability" of glasses. However, as some of the common optical glasses are known to possess poor chemical durability over a wide range of conditions [1],[1] but still render excellent service, it is evident that many of the methods

[1] Figures in brackets indicate the literature references at the end of this paper.

687127—46——3

proposed for determining chemical durability [2] throw little or no light on the problem of serviceability. By far the largest percentage of optical glasses are exposed to the air throughout their life of service. Of the chemical constituents in the atmosphere that can affect glasses adversely, all of them generally react through an ionizing medium, of which water is the most familiar and one which is always present. From these simple considerations, general experience [3] and a limited quantity of contradictory data on the adsorption of water by glass [4], it appears probable that the hygroscopic nature of an optical glass is the primary factor with which serviceability is concerned.

II. EXPERIMENTAL PROCEDURE

The quantity of water vapor "sorbed" [2] [5] on a flat polished surface by many glasses is so slight that its magnitude cannot be readily determined by means of the ordinary analytical balance. In order to increase the exposed surface sufficiently to obtain adequate sensitivity, the glasses were crushed in a steel mortar and passed through a No. 150 sieve, 0.104-mm opening. A known quantity, approximately 1.5 g, of this powder dried at 110° C was then exposed in a shallow weighing bottle to controlled humidity conditions and the increase in weight obtained.

Several modifications of the exposure were tried:

1. A limited number of glasses of the binary series, Na_2O-SiO_2, K_2O-SiO_2, and Li_2O-SiO_2, were exposed in a glass desiccator vessel, the base of which was filled with distilled water. A uniform high humidity within this chamber was maintained by means of an aspirator drawing air through a Milligan gas-washing bottle filled with distilled water.

2. A set of glasses of the PbO-B_2O_3 series were exposed to 98-percent relative humidity obtained by a saturated solution of $CaSO_4.2H_2O$.[3]

3. A number of characteristic commercial glasses, including three typical optical glasses, were exposed to 95-percent relative humidity maintained by a saturated solution of $Na_2HPO_4.12H_2O$.[3]

In procedures 2 and 3 the humidity chamber was placed in an air bath thermostated at 25° C, and the atmosphere in the chamber itself was circulated by means of a small fan mounted in the ground-glass cover.

To make comparisons between glasses of different densities, the values are reported in terms of water sorbed per calculated equal surface exposed, i. e., water sorbed per cubic centimeter of powder, or stated in terms of known factors, water sorbed times density divided by weight of sample.

---

[2] Following the suggestion of McBain, the term "sorption" is used to express the results, regardless of the mechanism manifested. However, it is helpful in interpreting the data to remember that if equilibrium is not attained quickly one is not dealing with pure adsorption but also with a solution of the vapor in the interior of the solid (absorption) or an ordinary chemical reaction [6, p. 109].

[3] Although the relative humidities obtained by means of saturated salt solutions are not considered very reliable, they furnish an easy means of comparing the hygroscopicities of glasses on a relative basis. Causes of uncertainties lie in the difficulty of obtaining equilibrium rapidly and also in the sudden changes in realtive humidity arising at the moment a solution forms a crust over the surface.

III. RESULTS AND DISCUSSION

1. GLASSES OF FOUR BINARY SYSTEMS

(a) Na_2O-SiO_2, K_2O-SiO_2, Li_2O-SiO_2

The data plotted in figures 1, 2, and 3[4] show the water sorbed-percentage composition curves for glasses of the binary systems Na_2O-SiO_2, K_2O-SiO_2, and Li_2O-SiO_2, exposed from 1 to 6 days to the humidity maintained by the aspirator procedure. The results obtained and the composition of these glasses are listed with the respective

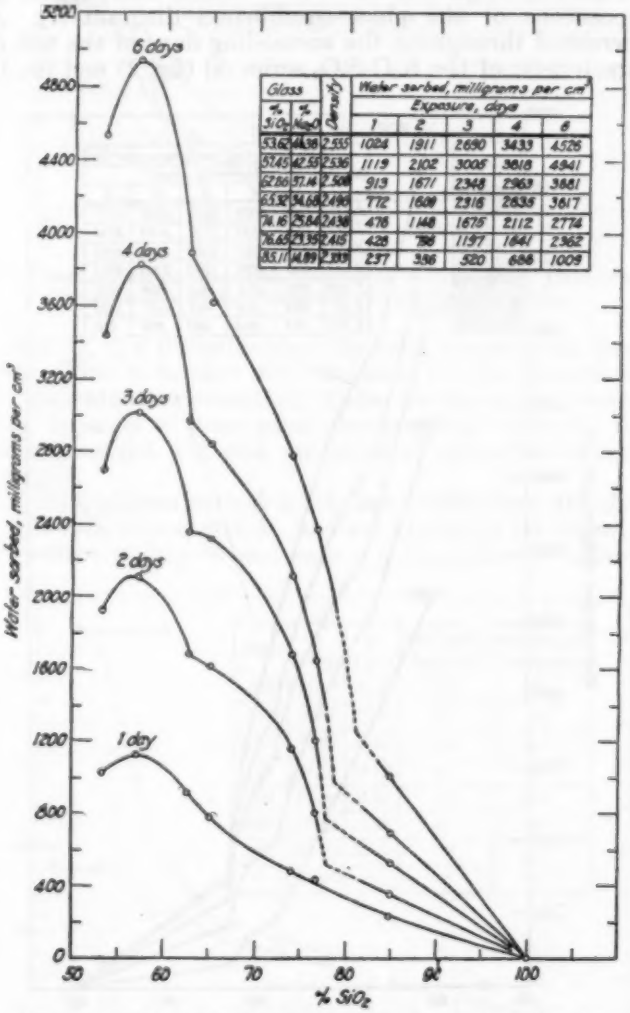

Glass		Density	Water sorbed, milligrams per cm²				
			Exposure, days				
% SiO_2	% Na_2O		1	2	3	4	6
53.62	46.38	2.555	1024	1911	2690	3433	4526
57.45	42.55	2.536	1119	2102	3005	3818	4941
62.86	37.14	2.508	913	1671	2348	2963	3881
65.32	34.68	2.496	772	1609	2316	2835	3617
74.16	25.84	2.438	476	1148	1675	2112	2774
76.65	23.35	2.415	428	798	1197	1641	2362
85.11	14.89	2.355	237	396	520	686	1009

FIGURE 1.—*Water sorbed by Na_2O-SiO_2 glasses as a function of their composition, after exposures of 1 to 6 days in the aspirator chamber.*

[4] Analyses made by F. W. Glaze of glasses prepared by C. A. Falck.

figures. All of the glasses of higher alkali content for the Na_2O-SiO_2 and K_2O-SiO_2 series became moist and some of them even went into solution. Nothing resembling an equilibrium value was attained after 6 days, indicating that true adsorption plays but a minor role and that absorption, reaction, and deliquescence are the predominating factors. The magnitude of the sorbed moisture correlates well with the known fact that the ability of these glasses to maintain a clear polished surface is very poor, but improves with increase in silica content.

For the Na_2O-SiO_2 series, the curve for composition plotted against water sorbed (fig. 1) gives indications of breaks that suggest the eutectic compositions of the phase-equilibrium diagram [7]. As these breaks persisted throughout the succeeding days of the test and were also characteristic of the K_2O-SiO_2 series [8] (fig. 2) and the Li_2O-SiO_2

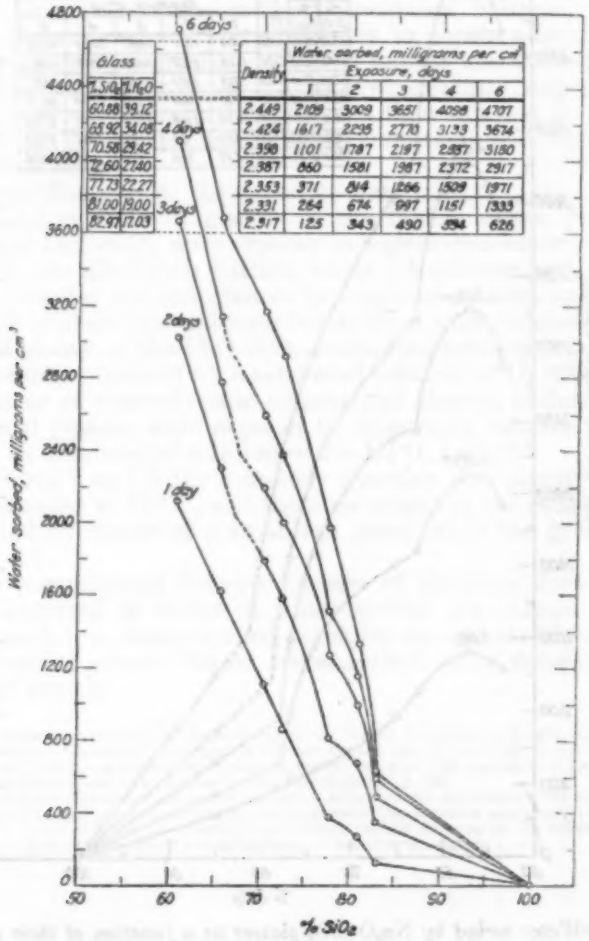

Glass		Density	Water sorbed, milligrams per cm²				
			Exposure, days				
SiO_2	K_2O		1	2	3	4	6
60.88	39.12	2.449	2109	3009	3651	4098	4707
65.90	34.08	2.424	1617	2235	2770	3133	3674
70.58	29.42	2.398	1101	1787	2197	2557	3180
72.60	27.40	2.387	860	1581	1987	2372	2917
77.73	22.27	2.353	371	814	1266	1529	1971
81.00	19.00	2.331	264	674	997	1151	1333
82.97	17.03	2.317	125	343	490	594	626

FIGURE 2.—*Water sorbed by K_2O-SiO_2 glasses as a function of their composition, after exposures of 1 to 6 days in the aspirator chamber.*

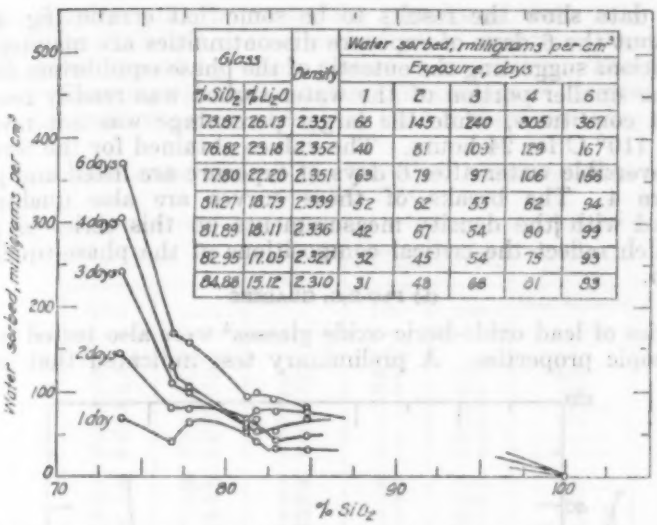

Glass		Density	Water sorbed, milligrams per cm² Exposure, days				
% SiO_2	% Li_2O		1	2	3	4	6
73.87	26.13	2.357	66	145	240	305	367
76.82	23.18	2.352	40	81	109	129	167
77.80	22.20	2.351	69	79	97	106	156
81.27	18.73	2.339	52	62	55	62	94
81.89	18.11	2.336	42	67	54	80	99
82.95	17.05	2.327	32	45	54	75	93
84.88	15.12	2.310	31	48	68	81	83

FIGURE 3.—*Water sorbed by* Li_2O-SiO_2 *glasses as a function of their composition, after exposures of 1 to 6 days in the aspirator chamber.*

series [9], (fig. 3), it is probable that the results have some qualitative significance. This is further substantiated by the observation that the breaks indicated are essentially those shown by the more precise data for the densities of these same glasses published by F. W. Glaze and his colleagues [10, 11], and for index of refraction on the Na_2O-SiO_2 glasses [12].

The Li_2O-SiO_2 glasses sorbed much less water than did the Na_2O-SiO_2 and K_2O-SiO_2 series, and, in fact are known to be far superior to the latter in their ability to maintain a clear surface. Although the

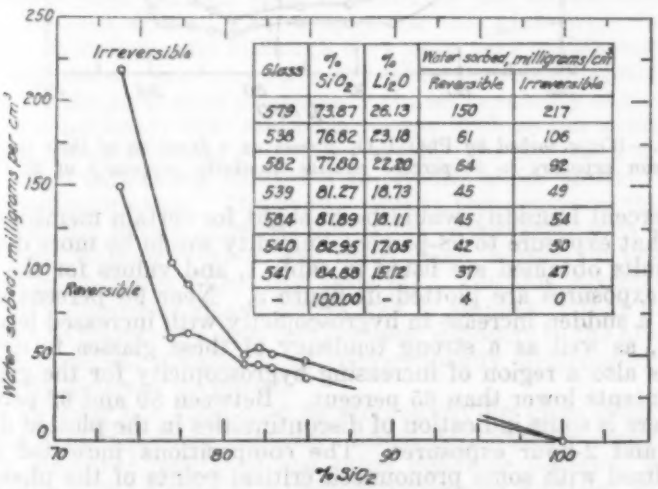

Glass	% SiO_2	% Li_2O	Water sorbed, milligrams/cm² Reversible	Irreversible
579	73.87	26.13	150	217
538	76.82	23.18	61	106
582	77.80	22.20	64	92
539	81.27	18.73	45	49
584	81.89	18.11	45	54
540	82.95	17.05	42	50
541	84.88	15.12	37	47
–	100.00	–	4	0

FIGURE 4.—*Reversible and irreversible water for* Li_2O-SiO_2 *glasses after 6 days of exposure in the aspirator chamber.*

plotted data show the results to be somewhat erratic (fig. 3), yet throughout the 6 days of exposure discontinuities are maintained at compositions suggesting the eutectic of the phase equilibrium diagram [9]. The smaller portion of the water sorbed was readily reversible at room conditions, while the larger percentage was not reversible even at 110° C for 24 hours. The values obtained for the reversible and irreversible water after 6 days of exposure are listed and plotted in figure 4. The breaks of these curves are also qualitatively in accord with the density measurements on this series of glasses [11], which reflect the critical compositions of the phase-equilibrium diagram.

(b) PbO-B_2O_3 GLASSES

A series of lead oxide-boric oxide glasses[5] were also tested for their hygroscopic properties. A preliminary test indicated that sorption

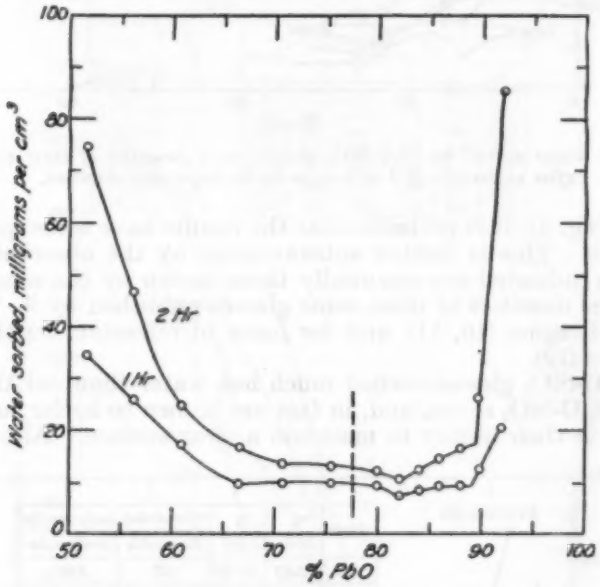

Figure 5.—*Water sorbed by* PbO–B_2O_3 *glasses as a function of their composition upon exposure to 98-percent relative humidity (approx.) at 25°C.*

at 95-percent humidity would be so slight for certain members of the group that exposure to 98-percent humidity would be more desirable. The results obtained are listed in table 1, and values for the 1- and 2-hour exposures are plotted in figure 5. Near 90 percent of PbO there is a sudden increase in hygroscopicity with increased lead oxide content, as well as a strong tendency of these glasses to devitrify. There is also a region of increasing hygroscopicity for the glasses at PbO contents lower than 65 percent. Between 80 and 92 percent of PbO there is some indication of discontinuities in the plotted data for the 1- and 2-hour exposures. The compositions indicated can be rationalized with some pronounced critical points of the phase equi-

[5] Prepared and analyzed by Leo Shartsis in partial fulfillment of the requirements for the degree of Master of Arts, George Washington University, February 1942.

librium diagram [13]; however, the paucity of data and the complexity of the PbO-B_2O_3 system make further evidence desirable. Not all the water sorbed by these glasses is reversible. The glasses of extremes in composition retain a large percentage of the water sorbed in 16 hours, with the glass of highest PbO content retaining the most.

TABLE 1.—*Water sorbed (mg/cm² by PbO–B_2O_3 glasses at 98-percent relative humidity, 25° C*

Glass		Density [1]	Water sorbed during exposure for—		Irreversible water (at 110° C) after 16-hr exposure
PbO	B_2O_3		1 hr	2 hr	
Percent	*Percent*				
51.71	48.29	3.67	34.2	74.7	83.9
56.25	43.75	3.97	25.9	46.8	2.6
60.99	39.01	4.32	17.0	24.9	----------
66.50	33.50	4.76	9.7	16.6	0.9
70.70	29.30	5.12	9.9	13.2	----------
75.50	24.50	5.56	9.7	13.0	----------
79.93	20.07	5.99	9.3	12.0	----------
82.08	17.92	6.21	7.9	10.8	2.0
84.14	15.86	6.42	8.4	12.5	2.7
85.98	14.02	6.62	9.1	14.3	4.2
88.05	11.95	6.85	9.5	16.1	9.0
89.86	10.14	7.05	12.6	26.1	35.5
91.91	8.09	7.28	20.6	85.4	108.0

[1] Calculated by the equation $(\%\ PbO)^2/1600+2=$density [13].

2. COMPARISON OF SOME TYPICAL OPTICAL AND OTHER COMMERCIAL GLASSES

The results obtained on a group of typical glasses (composition, table 2) exposed to 95-percent relative humidity for 1-, 2-, 4-, and 16-hour periods are listed and plotted in figure 6. As these glasses could not all be tested at one time, the glass from a dish that had failed to maintain a clear surface upon exposure to the atmosphere was included in both series. The samples for this glass were from independent screenings, and although they gave very satisfactory checks, they undoubtedly give an overly optimistic picture of reproducibility. Hence, for the purpose of ascertaining the serviceability of an unknown glass, it is necessary that reference glasses, such as the unsatisfactory dish and the satisfactory goblet, be included for comparison.

The most interesting feature of the results is the position occupied by the optical glasses. The hygroscopicity test compares them favorably with the better chemical laboratory glasswares, such as Pyrex, Tamworth, Kimble N-51-A, and fused silica, a position they do not achieve in chemical durability tests [1]. Yet this juxtaposition of these very dissimilar glasses serves well to emphasize that the ability of a glass to maintain a clear surface upon exposure to the atmosphere, and its chemical durability as conventionally determined are two inherently different properties.

The Corning 015 glass used so successfully for glass electrodes [14] exhibits a high sorbing capacity, which undoubtedly contributes to its low electrical resistance and other desirable electrical properties [15, p. 78]. The glasses of intermediate sorbing capacity, such as the American Ceramic Society bottle No. 1 [16] window glass, etc., show

TABLE 2.—*Compositions (in percent) of some optical and other glasses tested for hygroscopicity*

[Calculated from batch compositions, unless otherwise noted]

Glass	Density	SiO_2	B_2O_3	P_2O_5	Al_2O_3	As_2O_3	Sb_2O_3	PbO	ZnO	CaO	MgO	BaO	K_2O	Na_2O	R_2O_3
Corning 015 [14, 15]	2.5	72.0								6.0				22.0	
Dish[a] (failed in service)	2.5	72.7		0.1	0.5	0.1	0.2			9.3		0.4		16.7	
Goblet[a]	2.8	66.1						17.2				1.4	9.7	5.6	
Electric hygrometer [17] (soft-glass tubing)	2.5														
Am. Ceram. Soc. bottle No. 1 [16]	2.5	73.3	Present		1.1					4.8	3.3		16.7		
Window glass	2.5	72.1								10.0	3.3			13.5	0.7
Blue bottle	2.5	77.5	0.5		3.5					5.6			12.9		
BSC 517	2.5	66.4	12.4			.5			0.5				11.8	8.4	
F 630	3.6	45.6				.5		45.1					5.2	3.6	
$PbO\text{-}B_2O_3$[b]	3.67		48.3					51.7							
BaC 572	3.20	49.7	3.6			.2	.4		7.2			30.8	7.7	.4	
Pyrex[c]	2.23	81.0	13.0			.002							.2	3.6	2.2
Fused silica	2.21	100													

[a] Glasses furnished by A. E. Williams.
[b] Analysis made by Leo Shartsis.
[c] Analysis made by Francis W. Glaze.

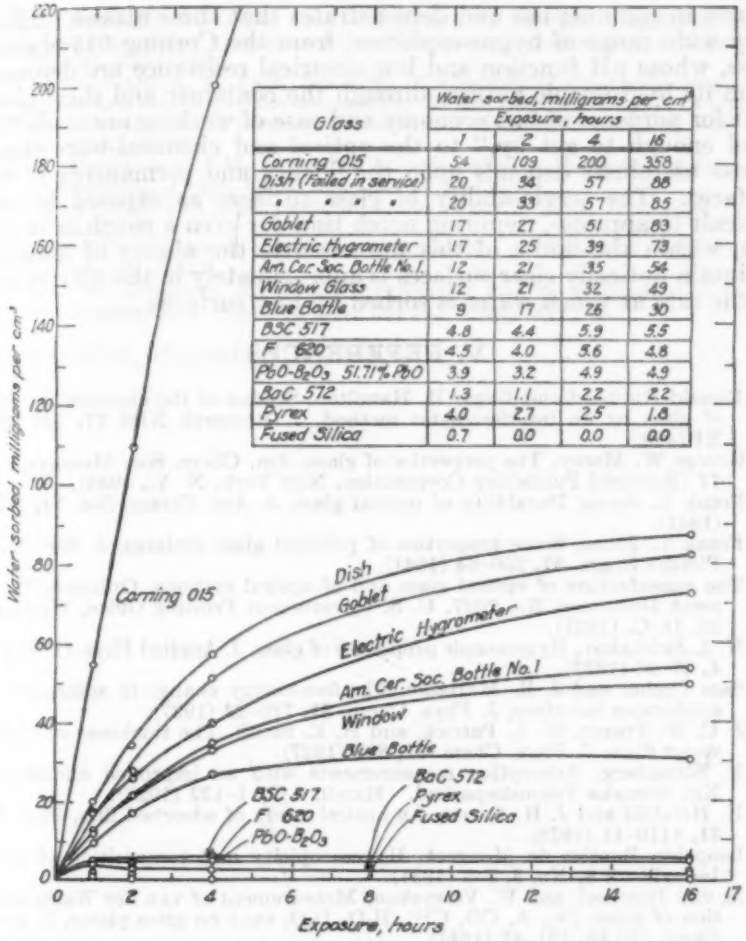

Glass	Water sorbed, milligrams per cm² Exposure, hours			
	1	2	4	16
Corning 015	54	109	200	358
Dish (Failed in service)	20	34	57	88
" " " "	20	33	57	85
Goblet	17	27	51	83
Electric Hygrometer	17	25	39	73
Am. Cer. Soc. Bottle No. 1.	12	21	35	54
Window Glass	12	21	32	49
Blue Bottle	9	17	26	30
BSC 517	4.8	4.4	5.9	5.5
F 620	4.5	4.0	5.6	4.8
$PbO-B_2O_3$ 51.7% PbO	3.9	3.2	4.9	4.9
BaC 572	1.3	1.1	2.2	2.2
Pyrex	4.0	2.7	2.5	1.6
Fused Silica	0.7	0.0	0.0	0.0

FIGURE 6.—*Comparison of optical and commercial glasses exposed to 95-percent relative humidity (approx.) at 25° C.*

reasonably satisfactory performance as glass electrodes but are not nearly so sensitive as the 015 glass. Further, the glasses that have very low sorption values are completely unsatisfactory for general glass electrode work, for example, the BaC 572, F 620, BSC 517, Pyrex, and fused silica.

IV. CONCLUSIONS

The powder hygroscopicity method has been tried on glasses covering a wide range of compositions and industrial uses. It offers considerable promise as a pertinent test for the serviceability of optical glasses, i. e., the ability to maintain a clear surface upon exposure to the atmosphere. It also possesses the unique advantages of simplicity and speed of determination. It readily differentiates between the

glasses in common use and demonstrates that these glasses exhibit a very wide range of hygroscopicities, from the Corning 015 electrode glass, whose pH function and low electrical resistance are dependent upon its hygroscopic nature, through the container and sheet glasses that for purposes of fuel economy and ease of working are made "just good enough to get by," to the optical and chemical-ware glasses, whose usefulness depends upon the fidelity and permanence of their surfaces. The serviceability of glass surfaces as exposed to air is difficult to appraise, requiring much time for even a rough estimation but, within the limits of this uncertainty, the ability of glasses to maintain optically clear surfaces is approximately in the inverse order to the rate at which water is sorbed by new surfaces.

V. REFERENCES

[1] Donald Hubbard and Edgar H. Hamilton, Studies of the chemical durability of glass by an interferometer method, J. Research NBS **27,** 143 (1941) RP1409.

[2] George W. Morey, The properties of glass, Am. Chem. Soc. Monograph No. 77 (Reinhold Publishing Corporation, New York, N. Y., 1938).

[3] Frank L. Jones, Durability of optical glass, J. Am. Ceram. Soc. **24,** 119–22 (1941).

Frank L. Jones, Some properties of polished glass surfaces, J. Soc. Motion Picture Engrs. **37,** 256–64 (1941).

The manufacture of optical glass and of optical systems, Ordnance Department Document No. 2037, U. S. Government Printing Office, Washington 25, D. C. (1921).

[4] N. A. Shishakov, Hygroscopic properties of glass, J. Applied Phys. (U. S. S. R.) **4,** 37–46 (1927).

Sam Lenher and J. R. McHaffie, The free-energy change in adsorption at a solid-vapor interface, J. Phys. Chem. **31,** 719–22 (1927).

J. C. W. Frazer, W. A. Patrick, and H. E. Smith, The thickness of adsorbed vapor films, J. Phys. Chem. **31,** 897 (1927).

R. Stromberg, Adsorption measurements with an improved microbalance, Kgl. Svenska Vetenskapsakad. Handl. **6** [2], 1–122 (1928).

K. Herzfeld and J. H. Frazer, An optical study of adsorbed film, Phys. Rev. **31,** 1110–11 (1928).

Leopaldo Buatier de Mongeot, Hygroscopicity and composition of glasses, Ind. silicati **8,** No. 3, 7–9 (1931).

A. van Itterbeek and W. Vereycken, Measurement of van der Waals adsorption of gases (N_2, A, CO, CH_4, H_2O, D_2O, etc.) on glass plates, Z. physik. Chem. [B] **48,** 131–47 (1941).

H. Menzel and S. Sliwinski, Studies on the system Li_2O-BeO-B_2O_3, Z. anorg. allgem. Chem. **249,** 337–385 (1942).

Stephen Brunauer, The adsorption of gases and vapors, **1** (Princeton University Press, 1943).

[5] James W. McBain, The mechanism of the adsorption ("sorption") of hydrogen on carbon, Phil. Mag. [6] 18, 916 (1909); Z. physik. Chem. **68,** 471 (1909).

[6] Herbert Freundlich, Colloid and capillary chemistry, English translation (E. P. Dutton & Co., Inc., New York, N. Y.).

[7] F. C. Kracek, The system sodium oxide-silica, J. Phys. Chem. **34,** 1583 (1930); J. Am. Ceram. Soc. **16,** 491 (1933).

[8] F. C. Kracek, N. L. Bowen, and G. W. Morey, The system potassium meta silicate-silica, J. Phys. Chem. **33,** 1857 (1929); J. Am. Ceram. Soc. **16,** 490 (1933).

[9] F. C. Kracek, The binary system lithium oxide-silica, J. Phys. Chem. **34,** 2641 (1930); J. Am. Ceram. Soc. **16,** 491 (1933).

[10] F. W. Glaze, J. C. Young, and A. N. Finn, The density of some soda-lime-silica glasses as a function of the composition, BS J. Research **9,** 799 (1932) RP507.

[11] J. C. Young, F. W. Glaze, C. A. Faick, and A. N. Finn, Density of some soda-potash-silica glasses as a function of the composition, J. Research NBS **22,** 453 (1939).
[12] C. A. Faick and A. N. Finn, The index of refraction of some soda-lime-silica glasses as a function of the composition, J. Am. Ceram. Soc. **14,** 518 (1931).
[13] R. F. Geller and E. N. Bunting, The system PbO-B_2O_3, J. Research NBS **18,** 585 (1937) RP995.
[14] D. A. MacInnes and M. Dole, The behavior of glass electrodes of different compositions, J. Am. Chem. Soc. **52,** 29–36 (1930).
[15] Malcolm Dole, The glass electrode (John Wiley & Sons, Inc., New York, N. Y., 1941).
[16] Report of Committee on the Chemical Durability of Glass, Bul. Am. Ceram. Soc. **14,** 181 (1935).
[17] Francis W. Dunmore, An electric hygrometer and its application to radio meteorography, J. Research NBS **20,** 723 (1938) RP1102.

WASHINGTON, December 19, 1945.

U. S. DEPARTMENT OF COMMERCE NATIONAL BUREAU OF STANDARDS

RESEARCH PAPER RP1707

Part of Journal of Research of the National Bureau of Standards, Volume 36, April 1946

SOLUBILITY OF CADMIUM SULFATE IN H_2O-D_2O MIXTURES

By Langhorne H. Brickwedde

ABSTRACT

The work reported here is a continuation of earlier studies on the effect of heavy water on the electromotive force of standard cells.

The solubility of cadmium sulfate was measured in heavy water and in normal water. This salt was found to be about 8 percent less soluble in heavy water than in normal water in the temperature range $-1°$ to $+70°$ C.

At 43.6° C, $CdSO_4 \cdot 8/3H_2O$, $CdSO_4 \cdot H_2O$, and saturated H_2O solution are in equilibrium. $CdSO_4 \cdot 8/3D_2O$, $CdSO_4 \cdot D_2O$, and saturated D_2O solution are in equilibrium at 45.4° C.

CONTENTS

	Page
I. Introduction	377
II. Measurements	377
III. Experimental results	378
IV. Comparison with other data in the literature	381
V. Summary	383
VI. References	383

I. INTRODUCTION

The solubility of cadmium sulfate in H_2O-D_2O mixtures was studied as a part of the work on standards of electromotive force dealing with the effect of D_2O on the electromotive force of standard cells. Two groups of cells described in earlier publications [1, 2] [1] have been made with mixtures of H_2O, HDO, and D_2O.

II. MEASUREMENTS

The solubility of cadmium sulfate was measured from $-1°$ to $+72°$ C in water that varied from 0.02 (normal water) to 99.5 mole percent D_2O. The experiments were made by continuously agitating crystals of cadmium sulfate in contact with the various aqueous solutions for periods varying from 24 to 300 hours. In most of the experiments 1- to 2-gram samples of the clear solution were removed for analysis. The $CdSO_4$ content was determined gravimetrically as $CdSO_4$ after heating the carefully dried sample in a muffle at 680° to 700° C in a stream of SO_3 gas. In a few experiments, those at 23.5° C, the composition of the saturated $CdSO_4$ solution was determined by

[1] Figures in brackets indicate the literature references at the end of this paper.

synthesis. Weighed amounts of $CdSO_4$ were added to a known weight of water until only a very small amount of the crystals remained undissolved after being shaken with the solution for 24 hours or longer.

Because cadmium sulfate dissolves very slowly, considerable attention was given to the matter of obtaining saturated solutions. At each temperature the salt was agitated continuously with the solution for very long periods of time—usually from several days to a week or longer. Further, from some solutions a second sample was taken for analysis after an additional shaking period of 20 hours. In some cases two flasks with the same solvent with different proportions of crystals and solution were agitated simultaneously, and the solutions from each were analyzed.

The solubility measurements for the monohydrate, $CdSO_4 \cdot H_2O$, at 29° and 72° C were made in a different way from the measurements described above. The solutions were allowed to remain in contact with $CdSO_4 \cdot H_2O$ crystals for 4 or 5 days and the flasks were shaken intermittently. The temperature varied by ±2 degrees centigrade. These data are much less precise than the other data of this report. They are included, however, because they greatly extend the temperature range of the monohydrate solubility curve.

Many of the earlier measurements above 40° C have not been included in the results reported here because of the uncertainty of which crystal hydrate was in contact with the solution. Above 40° C the solutions were saturated in ampules in a water bath controlled to ±0.05 degree because of the need of determining the hydrate transition temperature [3] and because of the greater change in solubility with temperature at the higher temperatures.

The deuterium content of the water was determined by density measurements after vacuum distillation of the samples. The volume was measured in a 0.4-milliliter pipette with calibrated inlet and outlet tubes. Weighings to ±10 micrograms were made on a high-precision balance by transposing the pipette and tare. The total deuterium content was calculated as D_2O, and is expressed throughout as mole percent D_2O of the water, although HDO was of course present.

The solubility measurements are reported for waters containing 0.02, 6.0, 50.0, 80.0, and 99.5 mole percent D_2O. In cases where the D_2O content varied slightly from these values, the solubility values were adjusted for the differences and are given for the five D_2O concentrations listed here.

III. EXPERIMENTAL RESULTS

The experimentally determined solubilities of cadmium sulfate, expressed as moles of $CdSO_4$ per mole of water, in normal water (0.02 mole percent D_2O), 6.0, 50.0, 80.0, and 99.5 mole percent D_2O are shown in figure 1 as they vary from −1° to +72° C.

From −1° to +43.6° C the crystal phase in stable equilibrium with an H_2O solution of cadmium sulfate is $CdSO_4 \cdot 8/3H_2O$. Above 43.6° the more stable crystal modification is $CdSO_4 \cdot H_2O$. The curves on the left in figure 1 represent the composition of solutions in equilibrium with $CdSO_4 \cdot 8/3aq$. The nearly parallel straight lines of the figure represent the composition of solutions in equilibrium with

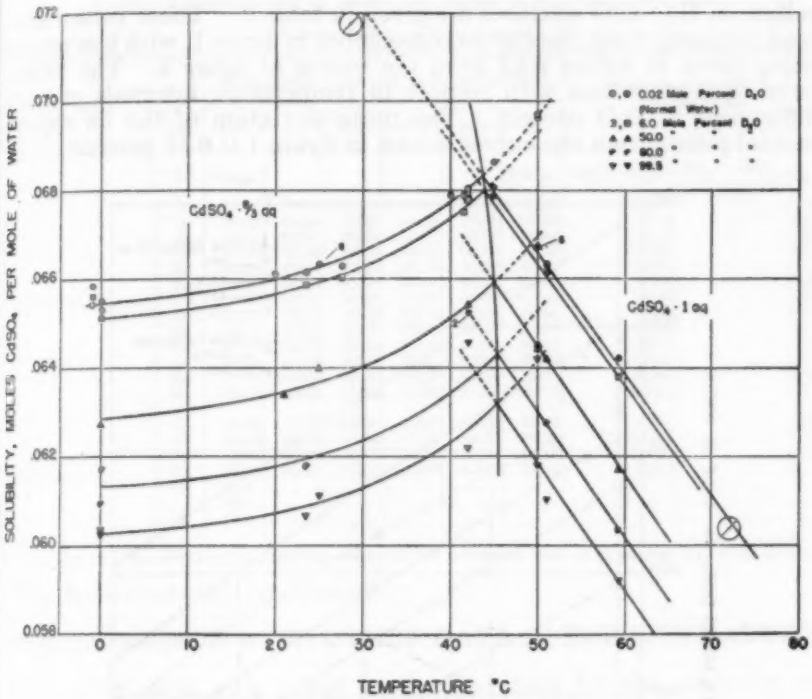

FIGURE 1.—*Solubility of cadmium sulfate in* H_2O-D_2O *mixtures.*

Numerals indicate number of observations represented by a single point.

$CdSO_4 \cdot 1aq$. The equilibrium temperature for $CdSO_4 \cdot 8/3H_2O$, $CdSO_4 \cdot H_2O$, and saturated H_2O solution is 43.6° C at atmospheric pressure. On the other hand, for $CdSO_4 \cdot 8/3D_2O$, $CdSO_4 \cdot D_2O$, and saturated D_2O solution the equilibrium temperature is 45.°4 C. These equilibrium temperatures and those for mixtures of the hydrate and deuterate are given in table 1. The temperatures are those of the intersections of the two solubility curves for each H_2O-D_2O mixture. The compositions of the saturated solution in equilibrium with the two crystal modifications are also given in table 1.

TABLE 1.—*Equilibrium temperatures for* $CdSO_4 \cdot 8/3aq$, $CdSO_4 \cdot 1aq$, *and saturated solution*

Composition of solvent, mole percent D_2O	0.02	6.0	50.0	80.0	99.5	100.
Equilibrium temperature, °C	43.6	43.9	45.0	45.3	45.4	45.4
Composition of saturated solution, moles of $CdSO_4$ per mole of water	0.06833	0.06803	0.06592	0.06430	0.06317	0.06314

The experimentally determined solubilities plotted with respect to temperature, shown in figure 1, are also plotted as a function of the D_2O content of the solvent in figure 2. Thirty points which can be read from each set of curves agree very closely, the mean deviation being 0.06 percent. The best values for the solubilities of cadmium

sulfate in H_2O-D_2O mixtures are given in table 2. These values were read primarily from the curves represented in figure 1, with less weight being given to values read from the curves of figure 2. The values have been smoothed with respect to temperature intervals and for differences in D_2O content. The mean deviation of the 68 experimental points from the curves shown in figure 1 is 0.16 percent.

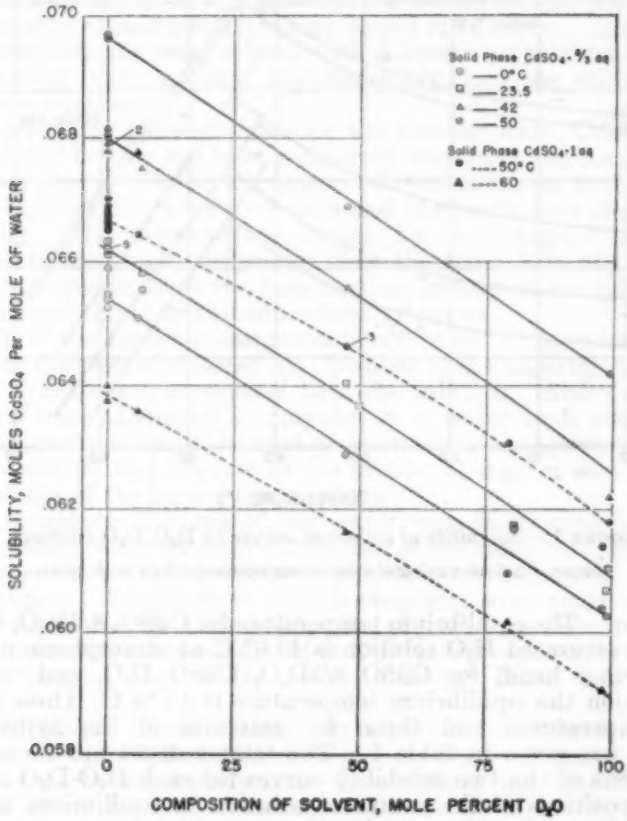

FIGURE 2.—*Isothermal lines for the solubility of cadmium sulfate in mixtures of* H_2O *and* D_2O.

Numerals indicate the number of observations represented by a single point.

The experimentally determined solubilities extrapolated to the solubility in 100 mole percent D_2O, designated as S_{D_2O}, are given in column 8 of table 2. The differences in solubility in H_2O and D_2O, $S_{H_2O}-S_{D_2O}$, are shown in column 9 and the percentage difference in column 10. The $CdSO_4$ content is about 8 percent less for $CdSO_4 \cdot 8/3D_2O$ in D_2O than for $CdSO_4 \cdot 8/3H_2O$ in H_2O. The $CdSO_4$ content is about 7.3 percent (6.9 percent at 45° and 7.7 percent at 60° C) less for $CdSO_4 \cdot D_2O$ in D_2O than for $CdSO_4 \cdot H_2O$ in H_2O.

TABLE 2.—*Solubility of cadmium sulfate in* H_2O-D_2O *mixtures*

[Moles of $CdSO_4$ per mole of water]

Solid phase	Temperature	Composition of solvent, mole percent D_2O						Difference of solubility in H_2O and D_2O	
		0.02	6.0	50.0	80.0	99.5	100		
	°C	[a]S_{H_2O}					[b]S_{D_2O}	$S_{H_2O}-S_{D_2O}$	$\frac{S_{H_2O}-S_{D_2O}}{S_{H_2O}}\times 100$
$CdSO_4$·8/3aq	0	0.06546	0.06511	0.06285	0.06131	0.06029	0.06026	0.00520	7.94
	5	.06555	.06520	.06294	.06138	.06036	.06033	.00522	7.96
	10	.06566	.06531	.06305	.06147	.06045	.06042	.00524	7.98
	15	.06580	.06545	.06319	.06159	.06058	.06055	.00525	7.98
	20	.06600	.06565	.06339	.06177	.06076	.06073	.00527	7.99
	23.5	.06619	.06584	.06358	.06194	.06093	.06090	.00529	7.99
	25	.06627	.06592	.06366	.06202	.06100	.06097	.00530	7.99
	30	.06663	.06627	.06402	.06236	.06133	.06130	.00533	7.99
	35	.06710	.06674	.06449	.06281	.06177	.06174	.00536	7.99
	40	.06773	.06737	.06512	.06342	.06235	.06232	.00541	7.99
	42	.06803	.06769	.06542	.06371	.06263	.06260	.00543	7.98
	45	.06857	.06823	.06594	.06423	.06314	.06311	.00546	7.96
	50	.06966	.06932	.06696	.06530	.06418	.06415	.00551	7.91
$CdSO_4$·aq	45	.06797	.06775	.06591	.06440	.06330	.06326	.00471	6.93
	50	.06659	.06638	.06448	.06299	.06185	.06181	.00478	7.18
	55	.06522	.06501	.06304	.06159	.06041	.06037	.00485	7.44
	60	.06385	.06363	.06159	.06019	.05897	.05893	.00492	7.71
	65	.0624	------	------	------	------	------	------	------
	70	.0611	------	------	------	------	------	------	------
	72	.0605	------	------	------	------	------	------	------

[a] S_{H_2O} denotes the solubility of cadmium sulfate in 100 percent of H_2O or in normal H_2O (0.02 percent D_2O).

[b] S_{D_2O} denotes the solubility in 100 percent D_2O.

IV. COMPARISON WITH OTHER DATA IN THE LITERATURE

No other data were found in the literature for the solubility of cadmium sulfate in D_2O. The solubilities of several other salts in D_2O have been reported, and these data are summarized in table 3. Except for $SrCl_2$, the difference in solubility in H_2O and D_2O of the other salts is of the same order of magnitude as for $CdSO_4$ in the temperature range of the present work.

TABLE 3.—*Comparison of solubility of* $CdSO_4$ *and some other salts in* H_2O *and* D_2O

Solid phase	Solubility in H_2O, S_{H_2O}	$\frac{S_{H_2O}-S_{D_2O}}{S_{H_2O}}\times 100$	Temperature	Authors
	Moles anhydrous salt per mole H_2O	*Percent*	°C	
$CdSO_4$·8/3H_2O	0.06543	7.94	0	National Bureau of Standards.
	.06708	7.99	40	Do.
$CdSO_4$·H_2O	.06797	6.93	45	Do.
	.06385	7.71	60	Do.
$CuSO_4$·5aq	.0173	13	5	Miles and Menzies [4].
	.0324	5.0	40	Do.
$CuSO_4$·3aq	.0847	1.7	95	Do.
	.0968	1.0	100	Do.
$SrCl_2$·6aq	.0502	0.4	0	Do.
	.0738	−1.7	40	Do.
$SrCl_2$·2aq	.0891	−3.8	55	Do.
	.1001	2.0	65	Do.
$SrCl_2$·aq	.1338	−0.3	125	Do.
	.1455	3.2	135	Do.
KCl	.0680	16.4	0	Shearman and Menzies [5].
	.0967	6.7	40	Do.
$BaCl_2$	.1723	1.8	160	Do.
	.0309	11.8	20	Taylor, Caley, and Eyring [6].
NaCl	.111	7.8	25	Do.
	.1107	5.4	25	Chang and Chu [7].

Chang and Chu [7] worked with NaCl in eight water mixtures from 0.02 to 99.59 mole percent D_2O. They found that the solubility of NaCl at 25° C decreased linearly with the increase in D_2O content of the water. Our data for $CdSO_4$ show that only at 0° and 50° C does a strictly linear relation hold. At the other temperatures in this investigation, 23.5° to 60° C, the curves are slightly concave downward (fig. 2).

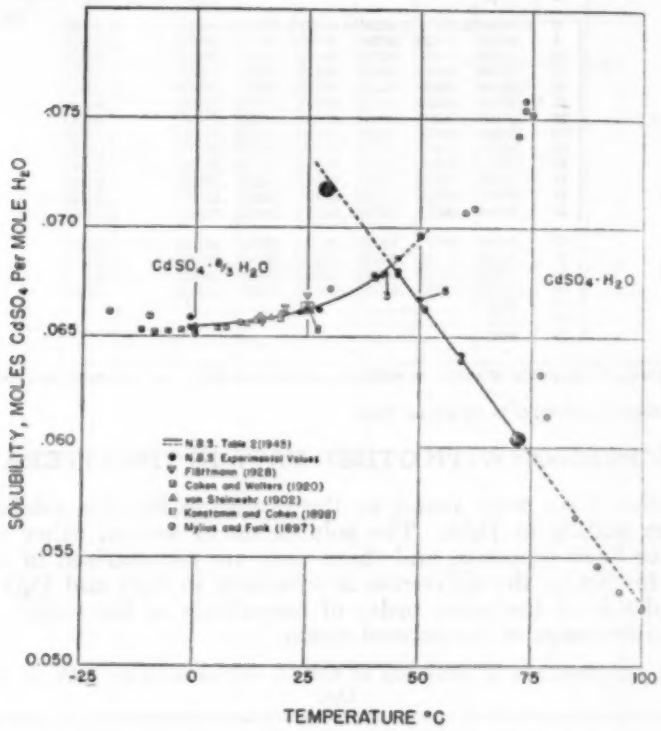

FIGURE 3.—*Solubility of cadmium sulfate in* H_2O *as given in the literature and from* NBS *measurements.*

The solubility of $CdSO_4$ in H_2O has been measured by a number of workers [8, 9, 10, 11, and 12]. Some of these determinations and the values reported here are represented in figure 3. The curves represent our best values for the solubility in H_2O as given in table 2. Below 40° C they are in good agreement with many of the earlier measurements. Because the earlier experimenters did not recognize the fact that the transition from the 8/3 hydrate modification to the monohydrate crystal occurred as low as 43.6° C and were working with the salt in a metastable condition, the earlier work deviates sharply from the values reported here at the higher temperatures. The occurrence of the transition between 43° and 44° C has been reported earlier [3]. In the earlier report, the equilibrium temperature for the two hydrates and the saturated solution was given as 43.4° C. The more extensive measurements reported here indicate that 43.6° is probably

a better value. The solubility data given in table 2 of this paper are also based on more extensive data than the values of the earlier report, from which they differ slightly.

V. SUMMARY

The solubility of cadmium sulfate in H_2O-D_2O mixtures varying from 0.02 to 99.5 mole percent D_2O has been determined over the temperature range $-1°$ to $+72°$ C. Values for the solubility of $CdSO_4 \cdot 8/3aq$ and $CdSO_4 \cdot 1aq$ are given for the various H_2O-D_2O mixtures. The $CdSO_4$ content of saturated solutions is about 8 percent less in D_2O than in H_2O.

The equilibrium temperature for $CdSO_4 \cdot 8/3aq$, $CdSO_4 \cdot 1aq$, and the saturated solution has been determined from the intersection of the solubility curves for the two crystal modifications. The equilibrium temperatures are 43.6° and 45.4° for H_2O and D_2O solvents, respectively.

The author gratefully acknowledges the assistance of Dr. George W. Vinal, under whose direction the work reported here was carried out.

VI. REFERENCES

[1] L. H. Brickwedde and G. W. Vinal, Electromotive force of saturated Weston standard cells containing deuterium oxide, J. Research NBS **20,** 599 (1938) RP1094.

[2] L. H. Brickwedde and G. W. Vinal, Relation of electromotive force to the concentration of deuterium oxide in saturated standard cells, J. Research NBS **27,** 479 (1941) RP1435.

[3] G. W. Vinal and L. H. Brickwedde, Metastability of cadmium sulfate and its effect on electromotive force of saturated standard cells, J. Research NBS **26,** 455 (1941) RP1389.

[4] F. T. Miles and A. W. C. Menzies, Solubilities of cupric sulfate and strontium chloride in deuterium water, J. Am. Chem. Soc. **59,** 2392 (1937).

[5] R. W. Shearman and A. W. C. Menzies, Solubilities of potassium chloride in deuterium water and ordinary water from 0° to 180° C, J. Am. Chem. Soc. **59,** 185 (1937).

[6] H. S. Taylor, E. R. Caley, and H. Eyring, The solubility of salts in H^2H^3O, J. Am. Chem. Soc. **55,** 4334 (1933).

[7] T. L. Chang and T. C. Chu, Solubility of sodium chloride in mixtures of hydrogen and deuterium oxides, Z. physik. Chem. [A]**184,** 411 (1939).

[8] Fr. Flöttmann, Solubility equilibria, Z. anal. Chem. **73,** 13 (1928).

[9] E. Cohen and J. J. Wolters, Die Temperaturformel des Westonchen Normalelements und die Löslichkeitskurve des $CdSO_4.8/3H_2O$, Z. physik. Chem. **96,** 253 (1920).

[10] H. von Steinwehr, Ueber den angeblichen Umwandlungspunkt des Cadmiumsulfat-Hydrats $CdSO_4.8/3H_2O$. Ann. Physik **314,** 1046 (1902).

[11] Ph. Kohnstamm and E. Cohen, Physikalisch-chemische Studien am Normalelement von Weston, Ann. Physik Chem. **65,** 344 (1898).

[12] F. Mylius and R. Funk. Ueber die Hydrate des Cadmiumsulfates, Ber. deut. chem. Ges. **30,** 824 (1897).

WASHINGTON, December 13, 1945.

U. S. DEPARTMENT OF COMMERCE NATIONAL BUREAU OF STANDARDS

RESEARCH PAPER RP1708

Part of Journal of Research of the National Bureau of Standards, Volume 36, April 1946

A GLOSSMETER FOR SMOOTHNESS COMPARISONS OF MACHINE-FINISHED SURFACES

By Richard S. Hunter

ABSTRACT

As shininess is one indication of surface smoothness, a photoelectric glossmeter was developed for possible use as a production-inspection device for evaluating the roughness of fairly coarse machine-finished surfaces. A near-grazing angle, 75 degrees, was chosen for the measurement of gloss. Therefore, specimens of the type having narrow ridges of metal between adjacent tool cuts are rated low in gloss, or *rough*. Although the glossmeter essentially measures the fraction of the unshadowed surface that is nearly parallel to mean surface, the instrument resulting from the present development has proved to be a simple and useful device for making rapid comparisons of the roughness of surfaces machined with about the same feeds.

CONTENTS

	Page
I. Introduction	385
II. The glossmeter	386
III. Use of the glossmeter	387
IV. Comparisons of glossmeter readings with root-mean-square deviations from mean surface	390
V. Summary	391

I. INTRODUCTION

Recently the National Bureau of Standards was asked by the War Department to suggest a rapid and simple production-inspection method for comparing the roughness of somewhat similar machine-finished surfaces. The roughness of the surfaces ranged between 100 and 500 microinches root-mean-square deviation from mean surface. The method was needed for identifying the rougher surfaces in this range that could not be rendered smooth by the application of single sprayed films of paint.

As shininess is one indication of surface smoothness, a photoelectric glossmeter was developed and tried for the purpose. A photoelectric reading of the gloss of a surface can be made quickly with this apparatus, which is inexpensive and does not damage the surface. Because the roughness involved is about one-thousand times as large as that which may affect the gloss of surfaces, every test surface has to be coated before gloss measurement with a liquid that will fill its microscopic cracks and pores. Without such a coating, it is impos-

sible to separate the gloss effects of microscopic irregularities from those of larger irregularities. The choice of a liquid for the purpose is described below.

II. THE GLOSSMETER

In planning the glossmeter, a near-grazing angle of specular reflection, 75 degrees, was chosen for two reasons: (1) low-gloss readings (indicative of coarseness) would thereby be given to any specimens having narrow ridges of metal extending appreciably above mean surface, and (2) the specular reflectance of the required coating liquid is much higher at this angle than the specular reflectance of the underlying metal surface covered with liquid; therefore, variation of the gloss of the underlying surface has relatively little effect on glossmeter reading.

In choosing the parts for the apparatus illustrated in figure 1, a barrier-layer photocell was selected because of the simplicity of the electrical equipment required with it. A standard five-cell flashlight lamp, which possesses a small concentrated filament, was chosen for the light source. A ⅝-inch lens having a focal length of 4 cm was selected because it provides a narrow beam of high flux density.

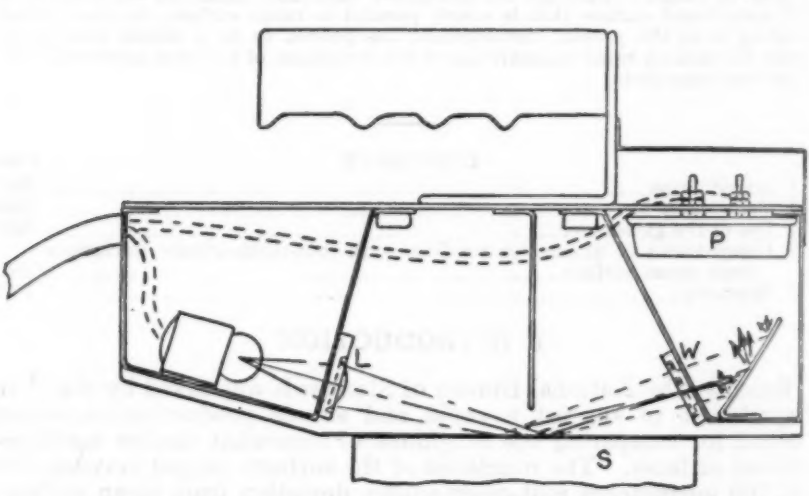

FIGURE 1.—*Vertical cross section of 75-degree glossmeter showing lens (L), specimen in position for measurement (S), window to photocell chamber (W), and barrier-layer photocell (P).*

In the glossmeter shown in figure 1, the converging beam from the lens is directed onto a machined surface at right angles to the tool marks. The light specularly reflected by the surface proceeds toward the photocell chamber. The small window at the entrance to this chamber admits only rays of reflected light whose average deviation from the direction of mirror reflection does not exceed 6.5 degrees. The interior of the chamber is coated white to conserve the light that enters.

The body of the instrument is built chiefly of duraluminum. With-

out handle, it is 25 by 8 by 4 cm in size. The grip handle makes the unit easy to position on specimens under test.

The control case (fig. 2) that accompanies the glossmeter contains a pointer-type galvanometer for registering photocell current, a 10-ohm rheostat for controlling the lamp current, a switch, and a small 110- to 6-volt transformer. As shown in figure 2, room is provided in the case for the glossmeter, connecting cable, and a small bottle of the liquid used to coat test surfaces.

The new glossmeter was designed primarily for measuring surfaces machined by lathe. The beam of light was restricted to small diameter so that test surfaces that are parts of cylinders or cones can be measured. As shown in figure 1, the plane of the test area must be placed in the plane of the bottom edges of the glossmeter. With cylindrical or conical test specimens of like size and shape, this placement may be conveniently obtained by attaching templates of the proper design to the sides of the glossmeter (see fig. 2).

III. USE OF THE GLOSSMETER

Values of 75-degree specular reflectance are proportional to deflections of the galvanometer. Polished black glass is a convenient standard to use with the instrument. The 75-degree specular reflectance of the average piece of black glass is 26 percent.[1]

Liquid-coated steel surfaces of the type being studied were found to reflect from 2 to about 25 percent of the incident beam into the photocell chamber. In using the glossmeter, an operator first places it on a clean, polished black-glass standard and adjusts the rheostat till the galvanometer registers a 26-division deflection. When this adjustment is made, values of specular gloss are read directly as deflections of the galvanometer.

The specular reflectances of 10 steel specimens machined in 8 different shops on lathes using feeds of from 0.017 to 0.025 inch were measured with the glossmeter. The root-mean-square roughness values of the same specimens were measured [2] with a Profilometer.[3] The surface of each test specimen was measured with both instruments at four selected areas. The results of these measurements are compared graphically in figures 3 and 4.

It proved difficult to find a coating liquid that would fill microscopic cracks and pores, without filling the larger cavities. The liquid necessarily had to have low surface tension and low viscosity. Kerosine and Stoddard solvent were first tried. A 90-second waiting period was required after Stoddard solvent was brushed generously onto a specimen so that the excess liquid could drain off and leave a film conforming to the major surface irregularities. As shown in figure 3, good separation of the machined surfaces according to their roughness was obtained with Stoddard solvent. Films of kerosine also performed satisfactorily, but a draining period longer than 90 seconds was required.

The draining period required after an application of Stoddard solvent or kerosine is objectionable in a method for production inspec-

[1] D. G. Moore and R. S. Hunter, Use of liquid surafces as standards of specular gloss, J. Am. Ceram. Soc. **24**, 167 (1941).
[2] By C. E. Haven, of the National Bureau of Standards Gage Section.
[3] E. J. Abbot, S. Bousky, D. E. Williamson, The Profilometer, Mech. Eng. **60**, 205 (1938).

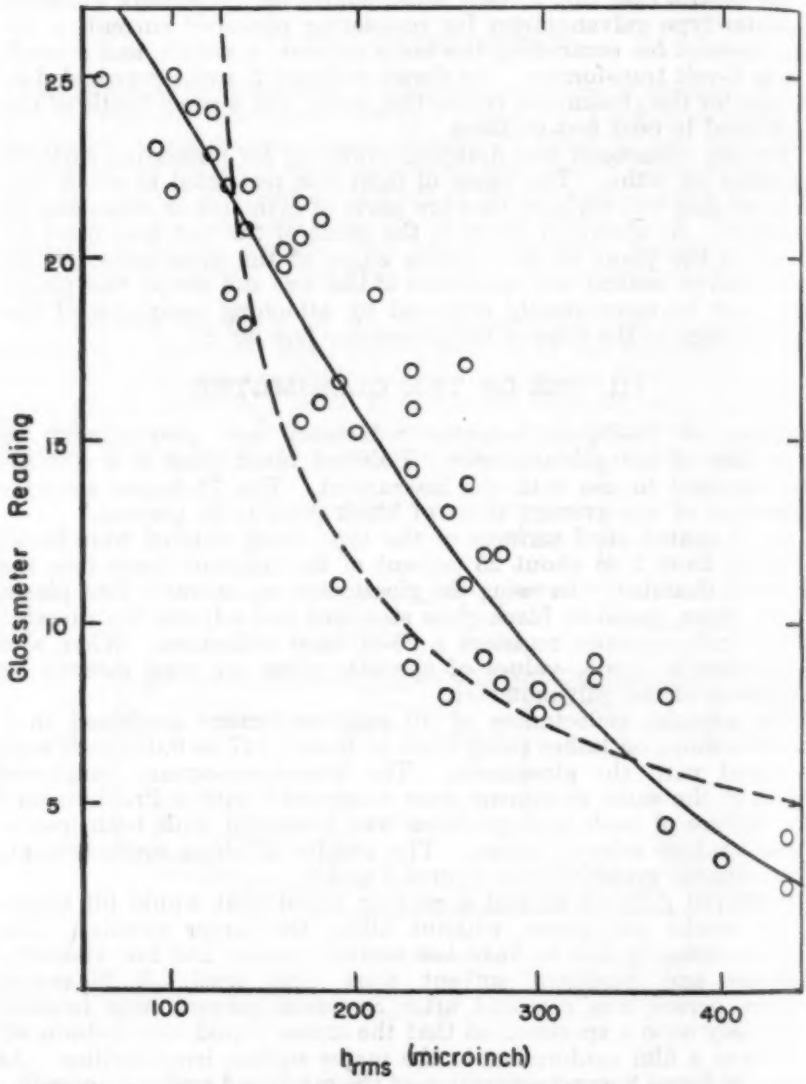

FIGURE 3.—*Relation between values of roughness measured with the Profilometer and those of gloss measured with the Stoddard solvent as the coating liquid.*

Measurements were made on steel specimens machined in 10 different shops. Dotted line represents relation computed for sine-shaped profile.

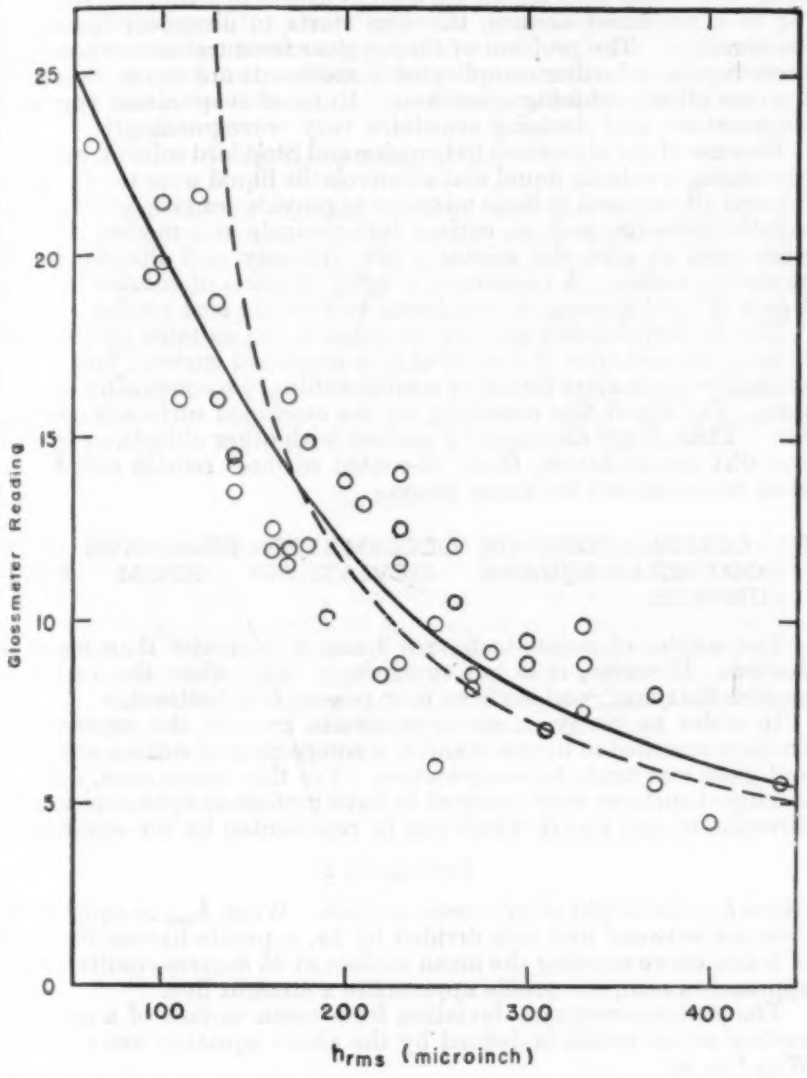

FIGURE 4.—*Relation between root-mean-square roughness measured with the Profilometer and gloss measured with mixture of light mineral oil and carbon tetrachloride as the coating liquids.*

Data were obtained from the same test areas as those plotted in figure 3. Dotted line represents relation computed for sine-shaped profile.

tion. In addition, there is only a brief period after draining in which the gloss values of such coated surfaces remain stable. Thus, about 30 to 45 seconds after the excess solvent drains to a thin film conforming to a machined surface, this film starts to disappear because of evaporation. The problem of timing gloss measurements when using these liquids is further complicated if specimens are warm, as is often the case after machining operations. Rates of evaporation vary with temperature, and draining schedules vary correspondingly.

Because of the objections to kerosine and Stoddard solvent, mixtures containing a volatile liquid and a nonvolatile liquid were tried. Light mineral oil was used in these mixtures to provide nonevaporating films; volatile solvents, such as carbon tetrachloride and methyl chloride, were used to give the mixtures low viscosity and therefore rapid spreading action. A mixture of roughly 10 parts of volatile liquid to 1 part of light mineral oil was found to give the best results.

The methyl-chloride mixture furnishes a film suitable for measurement 5 seconds after it is applied to a machined surface; the carbon-tetrachloride mixture furnishes a suitable film 20 seconds after application. The liquid film remaining on the machined surface is nonvolatile. Thus, if not damaged by contact with other objects, or by dust and dirt accumulation, these oil-coated surfaces remain suitable for gloss measurement for many hours.

IV. COMPARISONS OF GLOSSMETER READINGS WITH ROOT-MEAN-SQUARE DEVIATIONS FROM MEAN SURFACE

The scatter of points in figures 3 and 4 is greater than might be desired. However, it is not surprisingly large when the variety of profiles that machined surfaces may possess is considered.

In order to verify in an approximate manner the experimental findings recorded in figures 3 and 4, a comparison of surface roughness and gloss was made by computation. For this comparison, different machined surfaces were assumed to have profiles at right angles to the direction of tool travel, which can be represented by the equation

$$h = h_{max} \sin x,$$

where h is the height above mean surface. When h_{max} is equal to the distance between tool cuts divided by 2π, a profile having the shape of a sine curve crossing the mean surface at 45 degrees results; as h_{max} approaches zero, the profile approaches a straight line.

The root-mean-square deviation from mean surface of a machined surface whose profile is defined by the above equation was shown by Way [4] to be

$$h_{rms} = 0.708 h_{max}.$$

The value of specular gloss obtained from a machined surface with the present glossmeter is determined by the fraction of the surface reflecting light into the photocell chamber. The glossmeter was built to accept all light reflected within 6.5 degrees of the direction of

[4] S. Way, Description and observation of metal surfaces, Proc. special summer conference on friction and surface finish, p. 44, Massachusetts Institute of Technology, 1940. (Published by Murray Printing Co., Cambridge, Mass.).

reflection from a smooth surface. Because a reflected beam rotates twice as fast as the surface which reflects it, the only areas of a test surface that can thus direct light into the photocell chamber are those less than 3.25 degrees from parallel to the mean surface.

The fraction of the incident beam that is reflected into the photocell chamber by a machined surface measured across the direction of tool travel can be shown from the above considerations to be

$$R=\left(1-\frac{2}{\pi}\cos^{-1}0.0064\lambda/h_{\text{rms}}\right)R_{\text{max}},$$

where λ is the feed, or distance between tool cuts, and R_{max} is the reflectance that the coated metal surface would have if flat. The tool feeds for the steel specimens used in this study were about 0.020 inch. The glossmeter readings for the smooth steel specimens were found always to be 25 or 26. For these reasons, λ was made 0.020 inch and R_{max} was made 26 in computing the expected relation between gloss and h_{rms}. This relation is shown graphically by the dotted-line curve in figures 3 and 4. When the probable differences between actual profiles and assumed profiles are considered, the agreement between computed and observed data is considered reasonable.

V. SUMMARY

A glossmeter has been developed for use in comparing the roughness of machined surfaces. Although this instrument actually evaluates that fraction of surface area nearly parallel to mean surface not shaded by peaks, the instrument gives rapid and reasonably reliable comparisons of the roughness of different surfaces prepared with about the same tool feeds. Because glossmeter readings depend on the profile shapes rather than profile dimensions, the glossmeter is not a suitable instrument for roughness comparisons where tool feeds differ appreciably from specimen to specimen.

WASHINGTON, January 7, 1946.

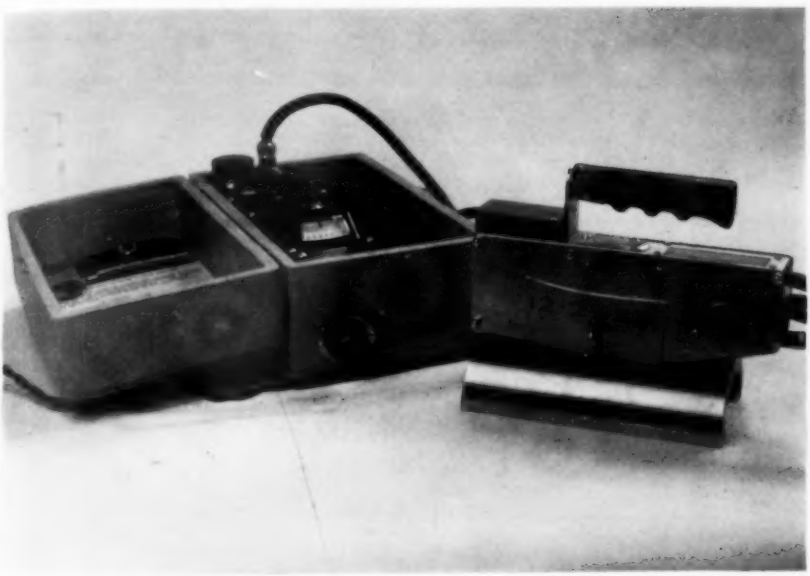

FIGURE 2.—*Glossmeter on specimen, and control box.*

U. S. Department of Commerce National Bureau of Standards

RESEARCH PAPER RP1709

Part of Journal of Research of the National Bureau of Standards, Volume 36, April 1946

ABSORPTION AND SCATTERING BY SOUND-ABSORBENT CYLINDERS

By Richard K. Cook and Peter Chrzanowski

ABSTRACT

The absorption and scattering of a plane wave of sound by an infinitely long circular cylinder whose axis is perpendicular to the direction of propagation of the wave are calculated. The surface of the cylinder is assumed to have a known normal acoustic impedance. The calculations take account of diffraction effects. Absorption measurements were made on long cylinders placed in a reverberation room, where the incident wave directions are at all angles to the axes of the cylinders, and were compared with the calculated values. In order to make the comparison, the reverberation-room statistics appropriate for cylinders (which are different from the statistics for flat patches of absorbent material) are developed and applied. The theory predicts, and measurements confirm, that absorbent cylinders can have coefficients of absorption greater than unity. Fairly good agreement between the calculated and measured coefficients is found. The reverberation-room statistics appropriate for spherical absorbers are also developed, although no measurements were made on spheres.

CONTENTS

	Page
I. Introduction	393
II. Wave field scattered by an absorbent cylinder	394
III. Absorption coefficient	396
IV. Statistics of reverberation-room wave fields	397
1. General	397
2. Flat absorber	398
3. Cylindrical absorber	399
4. Spherical absorber	401
V. Experimental results and discussion	402
1. Description of cylinders	402
2. Impedance measurements	402
3. Absoprtion measurements	403
VI. Experimental procedure	406
1. Impedance measurements	406
2. Absorption measurements	407
VII. Accuracy of measurements	408
VIII. Technic of calculation	409
IX. Summary	409
X. References	410

I. INTRODUCTION

Acoustic materials, which are used to reduce noise and control reverberation in rooms, are usually applied directly to walls and ceilings. Recently a manufacturer has developed an acoustic treatment that

consists of the installation of sound-absorbent material in the shape of long circular cylinders located at a distance from the walls. Rooms in which it is not possible to apply acoustic materials to the walls and ceilings can thus be treated acoustically.

In order to extend the absolute measurement of sound-absorption coefficients, it is important to study both theoretically and experimentally the absorption of cylinders having a known normal acoustic impedance. Owing to diffraction effects, the absorption is an entirely different function of frequency than is the absorption of a flat surface of the same material having an area equal to the peripheral area. Also, sound waves can approach a cylinder from all directions, whereas acoustic material on a flat wall can be approached by sound waves through a solid angle of only 2π. This means that the reverberation-room statistics for a cylindrical absorber will be different from those for a flat patch of absorbent material on the wall.

II. WAVE FIELD SCATTERED BY AN ABSORBENT CYLINDER

Consider the absorption and scattering of a plane single-frequency wave by an infinitely long circular cylinder of sound-absorbent material whose axis is assumed to be perpendicular to the direction of propagation of the wave. The ratio of sound pressure at a point on the surface to the component of particle velocity normal to the surface is assumed to have a constant value, the normal impedance Z, independent of location of the point on the surface. This is equivalent to assuming that the acoustic effects of motion of a point on the surface are transmitted to other points on the surface only through the surrounding air and not through the body of the cylinder.

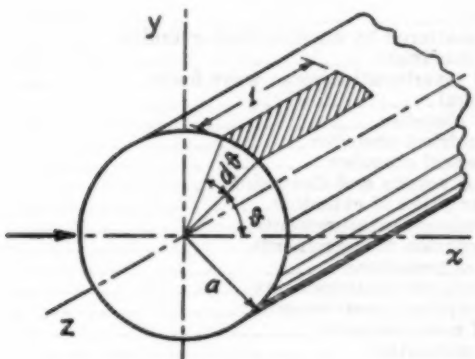

FIGURE 1.—*Representation of absorbent cylinder.*

If the distributions of sound pressure and particle velocity are independent of z (incident wave fronts parallel to the z-axis, which coincides with the axis of the cylinder, as shown in fig. 1), what is the scattered wave field?

Let k be the generalized wave number of the incident plane wave, and let ω be the generalized angular velocity. Then the velocity potential is

$$\Phi_i = \phi_0 e^{i(\omega t - kx)} = \phi_0 e^{i(\omega t - kr\cos\vartheta)}$$

$$= \phi_0 \left[J_0(kr) + 2 \sum_{\mu=1}^{\infty} (-i)^\mu J_\mu(kr) \cos \mu\vartheta \right] e^{i\omega t} \tag{1}$$

and there is no loss of generality in supposing $\phi_0 = 1$. This well-known expansion of Φ_i in a series of Bessel functions $J_\mu(kr)$ is convergent for all values of r and ϑ. The introduction of Bessel functions facilitates satisfaction of the boundary conditions at the surface of the absorbent cylinder.

Besides the incident wave there is a wave scattered by the cylinder. A function which satisfies the wave equation and which represents an outgoing wave, as can be seen by its asymptotic expansion for large r, is $[J_\mu(kr) - iY_\mu(kr)]e^{i\omega t} \cos \mu\vartheta$. The function $Y_\mu(kr)$ is the other solution of Bessel's differential equation, as defined in Whittaker and Watson's "Modern Analysis." This function is sometimes denoted by $N_\mu(kr)$. The entire expression $J_\mu(kr) - iY_\mu(kr)$ is Hankel's function $H_\mu^{(2)}(kr)$.

Hence a general expression for the velocity potential of the scattered wave is

$$\Phi_s = \sum_{\mu=0}^{\infty} b_\mu (J_\mu - iY_\mu) e^{i\omega t} \cos \mu\vartheta. \tag{2}$$

The b_μ's are constants to be determined by the boundary conditions at the surface of the cylinder, and the Bessel functions J_μ and Y_μ are understood to be functions of kr. Terms involving $\sin \mu\vartheta$ do not appear, as can be seen from considerations of symmetry.

The total velocity potential due to both incident and scattered waves is $\Phi = \Phi_i + \Phi_s$. The total sound pressure at any point is $p = -\rho(\partial\Phi/\partial t)$, ($\rho$=density of air) and the radial velocity component, which is normal to the surface of the cylinder, is $v_r = (\partial\Phi/\partial r)$. The boundary condition at the surface of the cylinder is

$$p = -Zv_r, \ (r = a), \tag{3}$$

where the constant Z is the usual normal impedance. The negative sign must be used because the positive direction of v_r is *out* of the absorbent surface ,whereas it is customary to measure the impedance Z with the positive direction for particle velocity *into* the absorbent surface.

Calculation of p and v_r from the total velocity potential Φ and substitution into eq 3 yield the following equations for determination of the b_μ's:

$$\left.\begin{aligned} &-\frac{Z}{\rho c}[J_0' + b_0(J_0' - iY_0')] + i[J_0 + b_0(J_0 - iY_0)] = 0 \\ &-\frac{Z}{\rho c}[2(-i)^\mu J_\mu' + b_\mu(J_\mu' - iY_\mu')] + i[2(-i)^\mu J_\mu + b_\mu(J_\mu - iY_\mu)] = 0 \\ &\mu = 1, 2, 3, \ldots, \end{aligned}\right\} \tag{4}$$

in which it is understood that $J_\mu = J_\mu(ka)$, $J'_\mu = \frac{dJ_\mu(ka)}{d(ka)}$, and similarly for J_0, J'_0, Y_0, Y'_0, Y_μ, Y'_μ. The quantity c is the velocity of sound. After the b_μ's are computed from eq 4, substitution into eq 2 will yield the final expression for the velocity potential of the wave scattered by the absorbent cylinder. The scattered wave potential has possible applicatons in the design of dead rooms and reverberation rooms.

III. ABSORPTION COEFFICIENT

The total time-averaged acoustic power, P, absorbed by unit length of the cylinder from the incident plane wave can be readily computed with the help of the b_μ's given in eq 4.

Let p and v_r, both functions of ϑ, be the sound pressure and the normal component of particle velocity, respectively, at a point on the surface of the cylinder (see fig. 1). Then the force due to the sound field on the shaded strip shown in figure 1 is $-apd\vartheta$. In complex notation,

$$p=|p|e^{i(\omega t+\phi_1)},\ v_r=|v_r|e^{i(\omega t+\phi_2)}, \tag{5}$$

where ϕ_1 and ϕ_2 are phase angles. Therefore, the time-averaged power, dP, of the force $-apd\vartheta$ causing the velocity v_r is

$$dP=-\tfrac{1}{2}|p|\ |v_r|a\cos(\phi_1-\phi_2)d\vartheta \tag{6}$$

By hypothesis, $p=-Zv_r$, and if $Z=|Z|e^{i\delta}$, then $\phi_1-\phi_2=\pi+\delta$. Substitution into eq 6 and integration yield for the total time-averaged power absorbed by unit length of the cylinder

$$P=\frac{a\cos\delta}{2|Z|}\int_0^{2\pi}|p|^2d\vartheta. \tag{7}$$

The Fourier series for p can be written

$$p=\sum_{\mu=0}^{\infty}a_\mu e^{i\omega t}\cos\mu\vartheta, \tag{8}$$

in which the a_μ's are, in general, complex numbers.

Substitution of eq 8 into eq 7 yields

$$P=\frac{\pi a\cos\delta}{|Z|}\left\{|a_0|^2+\tfrac{1}{2}\sum_{\mu=1}^{\infty}|a_\mu|^2\right\} \tag{9}$$

The a_μ's are found by computing p from the total velocity potential.

$$\left.\begin{aligned} a_0&=-i\omega\rho[J_0+b_0(J_0-iY_0)]\\ a_\mu&=-i\omega\rho[2(-i)^\mu J_\mu+b_\mu(J_\mu-iY_\mu)]\\ \mu&=1,\ 2,\ 3,\ \ldots. \end{aligned}\right\}, \tag{10}$$

in which, just as in eq 4, it is understood that $J_\mu = J_\mu(ka)$, etc. Substitution of the values of b_μ obtained from eq 4 into these equations gives

$$\left.\begin{aligned} |a_0|^2 &= \frac{4|Z|^2}{\pi^2 a^2} \cdot \frac{1}{\left|-\frac{Z}{\rho c}(J_0' - iY_0') + i(J_0 - iY_0)\right|^2} \\ |a_\mu|^2 &= \frac{4|Z|^2}{\pi^2 a^2} \cdot \frac{4}{\left|-\frac{Z}{\rho c}(J_\mu' - iY_\mu') + i(J_\mu - iY_\mu)\right|^2} \end{aligned}\right\} \tag{11}$$

Finally, a definition of absorption coefficient is needed. The time-averaged acoustic power transmitted by the incident plane wave through unit area is $P_0 = \omega\rho k/2$. The power absorbed per unit peripheral area of the cylinder is $P/2\pi a$. We define the absorption coefficient α_p for a plane wave incident normally to the axis by

$$\alpha_p = \frac{P}{2\pi a P_0}. \tag{12}$$

It is shown in section IV that the random incidence effective absorption coefficient for a cylinder measured in a reverberation room is greater than α_p by a factor of π if the Sabine reverberation formula is used to compute absorption coefficient from measured decay times. We define the reverberation-room absorption coefficient α_r by

$$\alpha_r = \pi\alpha_p = \frac{P}{2aP_0} \tag{13}$$

Both α_p and α_r are expressed in sabins per unit peripheral area.

The final expression for the reverberation room absorption coefficient is

$$\alpha_r = \frac{4}{\pi}\frac{|Z|\cos\delta}{\rho c}\left(\frac{1}{ka}\right)^2\left\{\frac{1}{\left|-\frac{Z}{\rho c}(J_0' - iY_0') + i(J_0 - iY_0)\right|^2} + \sum_{\mu=1}^{\infty}\frac{2}{\left|-\frac{Z}{\rho c}(J_\mu' - iY_\mu') + i(J_\mu - iY_\mu)\right|^2}\right\}. \tag{14}$$

With known values of Z and suitable tables of Bessel functions, one can compute the absorption coefficient of a cylinder by means of this equation.

IV. STATISTICS OF REVERBERATION ROOM WAVE FIELDS

1. GENERAL

An absorbent cylinder placed at a distance from the walls of a reverberation room is approached by sound waves from all directions, whereas a flat patch of absorbent material on the wall of a reverbera-

tion room can be approached by sound waves coming through a solid angle of only 2π. This will give rise to a difference in the reverberation-room statistics, by means of which coefficients of sound absorption are deduced from measurements of decay time. In order to emphasize the differences, the statistics for a flat patch of absorbent material will be briefly given. A technic of calculation in which plane waves are handled statistically is introduced in order to include diffraction effects in a logical way. This technic is different from those used by Jäger [1] [1] and Buckingham [2]. In addition, the statistics for cylinders and spheres will be developed.

Throughout the discussion, the following assumptions will hold: (1) The wave motion in the reverberation room of volume V is completely random. At every point within the room, plane waves of all directions and phases will have passed by after a sufficiently long time (short, however, in comparison with the reverberation time) has elapsed. The plane wave in any given cone of directions, of solid angle $d\Omega$, is assumed to have the same average intensity as every other plane wave. As a corollary, the energy density, W, is the same at every point within the room. (2) In the statistical calculations, plane waves incident on the absorber are associated with elements of area, $R^2 d\Omega$, located on a spherical surface of integration whose center is at the absorber. The time-averaged intensity of an incident plane wave associated with such an element of area is assumed to be directly proportional to the solid angle $d\Omega$ subtended by the area at the absorber. (3) At any given instant, there might be a number of plane waves incident on the sound absorber. The rate of absorption of energy by the cylinder or sphere, or patch on the wall, is assumed to be the sum of the rates for the individual plane waves. This is equivalent to assuming that, on the average, no power is developed at the absorbing surface by the sound pressure of one incident plane wave acting on the particle velocity of another incident plane wave.

The first assumption fixes the statistical distribution of the sound waves incident upon the absorber. The third assumption is basically the rule of superposition for rates of absorption. It is a considerable advantage to have such a rule, as the calculation of rates of absorption for plane waves is in general much simpler than for any other kind of incident wave.

A corollary of the first two assumptions is that the time-averaged intensity of the plane wave coming from any direction is $Wcd\Omega/4\pi$.

2. FLAT ABSORBER

Suppose a flat patch of absorbent material is placed on the wall of the reverberation room (see fig. 2). Let the effective area of the patch be A_f for a plane wave at normal incidence. A_f is the product of the geometrical area of the patch and its absorption coefficient. The product of A_f and the intensity gives the rate of absorption of sound energy from the plane wave. A_f will include the effects of diffraction near the edges of the patch, and might be either greater or less than the geometrical area of the patch. For a plane wave at angle of incidence ϑ, the effective area is assumed to be $A_f \cos \vartheta$.

[1] Figures in brackets indicate the literature references at the end of this paper.

Then the rate of absorption of sound energy by the patch is

$$P_f=\int_0^{\frac{\pi}{2}}\int_0^{2\pi} A_f\cos\vartheta\frac{WcR^2\sin\vartheta\,d\phi d\vartheta}{4\pi R^2}$$

$$=\frac{A_fWc}{4} \tag{15}$$

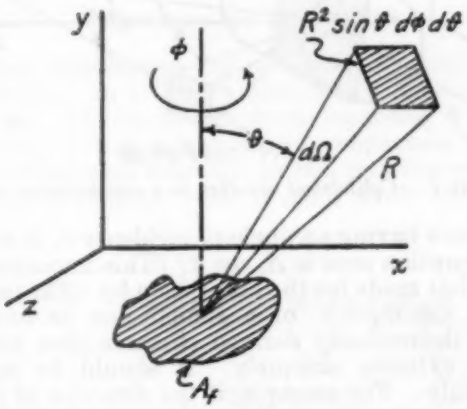

FIGURE 2.—*Flat absorber on the wall of a reverberation room.*

Hence the differential equation for the decay of sound in the room and its solution are

$$V\frac{dW}{dt}+\frac{A_fc}{4}W=0,\quad W=W_0e^{-\left(\frac{A_fc}{4V}\right)t} \tag{16}$$

Finally, if T is the time required for W to decay by a factor of e, then

$$A_f=\frac{4V}{cT}. \tag{17}$$

This is the Sabine expression generally used for calculation of absorption coefficients from reverberation-room measurements of decay time.

3. CYLINDRICAL ABSORBER

Suppose an absorbent cylinder, of length l great enough so that end effects can be neglected, is placed at a distance from the walls of the reverberation room. Let the effective area of the cylinder be A_c (see fig. 3) for a plane wave whose direction of propagation is perpendicular to the axis of the cylinder. The product of A_c and the intensity gives the rate of absorption of sound energy from the plane wave. It is clear that $A_c=2\pi al\alpha_p$, where α_p is as defined in section III. As A_c includes the effects of diffraction (computed in section III), it might be either greater or less than the geometrical area $2al$ of the actual cylinder projected on the plane wave front. The cylinder shown in figure 3 is formed by revolving A_c about the axis of the actual absorbent cylinder.

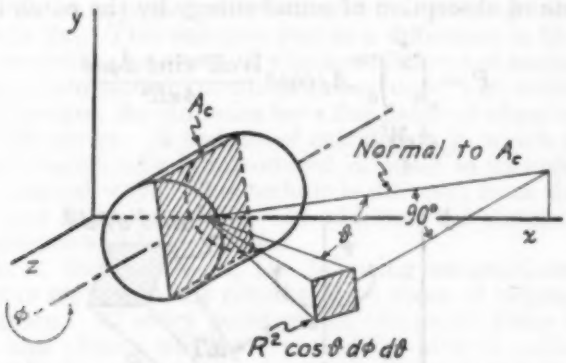

FIGURE 3.—*Cylindrical absorber in a reverberation room.*

For a plane wave having an angle of incidence ϑ, it is assumed that the effective absorption area is $A_c \cos \vartheta$. This important assumption is analogous to that made for the absorption by a flat patch at oblique incidence. The assumption, or a similar one, is necessary in the absence of any theoretically derived effective area for plane waves that strike the cylinder obliquely. It should be regarded as an approximation only. For example, if the direction of propagation of the incident plane wave is parallel to the axis of the cylinder, then $A_c \cos \vartheta = 0$, which is evidently not true.

The rate of absorption of sound energy by the cylinder is

$$P_c = \int_{-\frac{\pi}{2}}^{\frac{\pi}{2}} \int^{2\pi} A_c \cos \vartheta \frac{WcR^2 \cos \vartheta \, d\phi \, d\vartheta}{4\pi R^2}$$

$$= \pi \frac{A_c W c}{4} \tag{18}$$

If, as before, T is the time required for W to decay by a factor of e, then

$$A_c = \frac{1}{\pi} \frac{4V}{cT}. \tag{19}$$

The right-hand side of this equation differs from that of the Sabine expression, eq 17, by the factor $1/\pi$. It would be advantageous to express the absorption coefficient and effective absorption area for cylinders in units such that the Sabine formula could be used to compute decay time. Therefore, we define the random incidence effective absorption area A_r by

$$A_r = \pi A_c = \frac{4V}{cT}. \tag{20}$$

Finally, the reverberation-room absorption coefficient α_r (introduced in eq 13) is

$$\alpha_r = \frac{A_r}{2\pi a l} = \frac{1}{2\pi a l} \frac{4V}{cT}. \tag{21}$$

The foregoing explains the statement made in section III (compare eq 12 and 13) that the effective absorption coefficient of a cylinder in a reverberation room is π times as great as the absorption coefficient for a plane wave incident normally to the axis. Section V contains the results of experiments designed to furnish a comparison between values of α_r computed from the normal impedance (eq 14) and values measured in a reverberation room (eq 21).

4. SPHERICAL ABSORBER

The statistical calculations for spherical absorbers do not suffer from the defect that an arbitrary assumption must be made, as was made for flat and cylindrical absorbers, regarding the absorption at oblique incidence. For this reason, the comparison between absorption coefficients computed from the normal impedance and coefficients measured in a reverberation room is more direct for spheres.

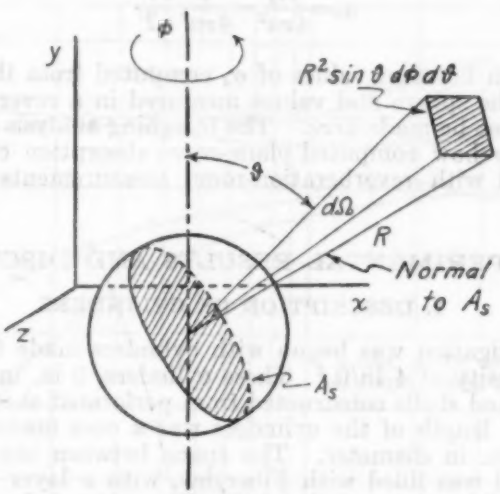

FIGURE 4.—*Spherical absorber in a reverberation room.*

Let the effective area of an absorbent sphere of radius a for a plane wave be A_s (see fig. 4). The product of A_s and the intensity gives the rate of absorption of sound energy from the plane wave. As for the flat patch and the cylinder, A_s includes the effects of diffraction and might be either greater or less than the geometrical area, πa^2, of the actual sphere projected on the plane wave front. The sphere shown in figure 4 is formed by revolving A_s about a diameter of the actual absorbent sphere.

The rate of absorption of sound energy by the sphere is

$$P_s = \int_0^{\pi}\int_0^{2\pi} A_s W c \frac{R^2 \sin\vartheta\, d\phi d\vartheta}{4\pi R^2}$$

$$= 4\,\frac{A_s W c}{4} \qquad (22)$$

If T is the time required for W to decay by a factor of e,

$$A_s=\frac{1}{4}\frac{4V}{cT}. \tag{23}$$

As for the absorbent cylinder, in order to express the absorption coefficient and effective area for spheres in units such that the Sabine formula can be used to compute decay time, we define the random incidence effective absorption area, A_t, by

$$A_t=4A_s=\frac{4V}{cT}. \tag{24}$$

The reverberation-room absorption coefficient α_t of a sphere is

$$\alpha_t=\frac{A_t}{4\pi a^2}=\frac{1}{4\pi a^2}\frac{4V}{cT}. \tag{25}$$

Comparison between values of α_t computed from the normal impedance of the sphere and values measured in a reverberation room (eq 25) will not be made here. The foregoing analysis is presented in order to show how computed plane-wave absorption coefficients can be correlated with reverberation-room measurements on absorbent spheres.

V. EXPERIMENTAL RESULTS AND DISCUSSION

1. DESCRIPTION OF CYLINDERS

The investigation was begun with cylinders made from Fiberglas having a density of 4 lb/ft.^{3} These cylinders, 9 in. in diameter and 97 in. long, had shells constructed from perforated sheet steel. Running the full length of the cylinders was a core made of perforated paper 5.75 in. in diameter. The space between the core and the cylinder shell was filled with Fiberglas, with a layer of scrim cloth between the Fiberglas and the shell. The ends of the cylinders were covered with perforated sheet metal.

Cylinders having one and two layers of cattle-hair felt were also investigated. From measurements on superposed layers and from measurements on the finished cylinders, it was found that the actual thickness of the felt was ⅞ in. The weight of the felt was 0.60 lb/ft.^{2} The cores for the felt-covered cylinders were 28-gage sheet-iron tubes, 4 in. in diameter and in sections approximately 10 ft long. After the first layer of felt was wrapped and the edges sewed together, the average radius of the finished cylinders was 2.88 in. The average radius after the second layer was added was 3.77 in.

2. IMPEDANCE MEASUREMENTS

Measurements of the normal acoustic impedance at the periphery of the Fiberglas cylinders were not feasible. Estimation of the impedance is difficult because of the perforated paper core. However,

the functional relationship

$$\frac{Z}{\rho c}=2-\frac{36}{13}\left(\frac{i}{ka}\right) \tag{26}$$

was assumed for the impedance on the basis of measurements reported by Beranek [3] for materials similar to the Fiberglas.

The results of normal impedance measurements for one and two layers of hair felt with rigid backing are shown in figure 5. Each plotted point represents the average of determinations on 15 samples selected at random from the original roll of felt. A modified Flanders [4] impedance tube was used to make the measurements. For both one and two layers of felt, the reactance curve at frequencies below 1,000 c/s is approximately that of a column of air having the same thickness as the felt.

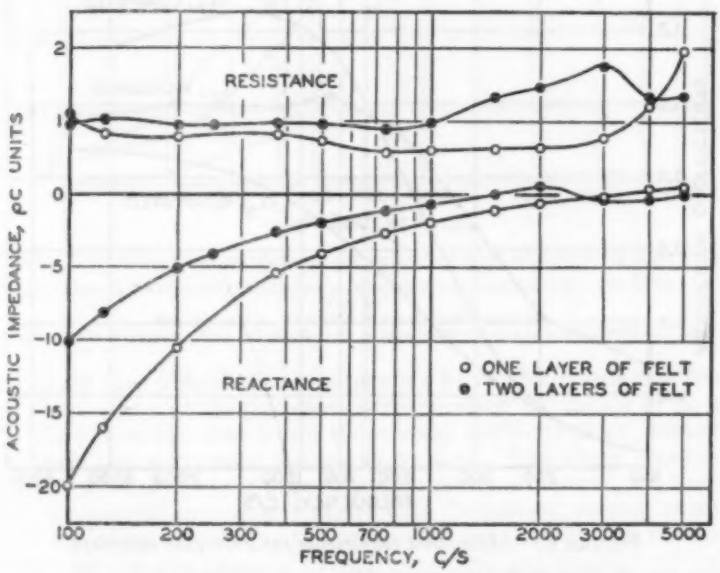

FIGURE 5.—*Impedance of hair felt for sound at normal incidence.*

3. ABSORPTION MEASUREMENTS

Reverberation-room measurements of the absorption coefficient α_r (defined by eq 21) were made on the Fiberglas cylinders and are plotted in figure 6. The absorption coefficients computed from the assumed impedance function (eq 26) by means of eq 14 are plotted in the same figure. We shall refer to these as the theoretical coefficients. The computed absorption coefficients α_n for normal incidence are also plotted. These are obtained by means of the usual equation

$$\alpha_n=1-\left|\frac{\frac{Z}{\rho c}-1}{\frac{Z}{\rho c}+1}\right|^2. \tag{27}$$

The curves show that diffraction effects at frequencies corresponding to values of ka near unity (480 c/s) result in absorption coefficients greater than 1. At high frequencies, where the wave length is short in comparison with the circumference ($ka>>1$), the cylinder will cast an acoustic shadow, and only the material on the side of the cylinder that faces the oncoming plane wave will be effective in absorbing sound. It is interesting to note that the theoretical value of α_r shows this shadow effect, because as the frequency rises above 1,000 c/s, α_r decreases even though α_s continues to increase. There is general agreement between the theoretical and measured reverberation-room values of α_r, although a critical comparison of the two sets of values cannot be made as the normal impedance values on which the calculations are based are only estimated.

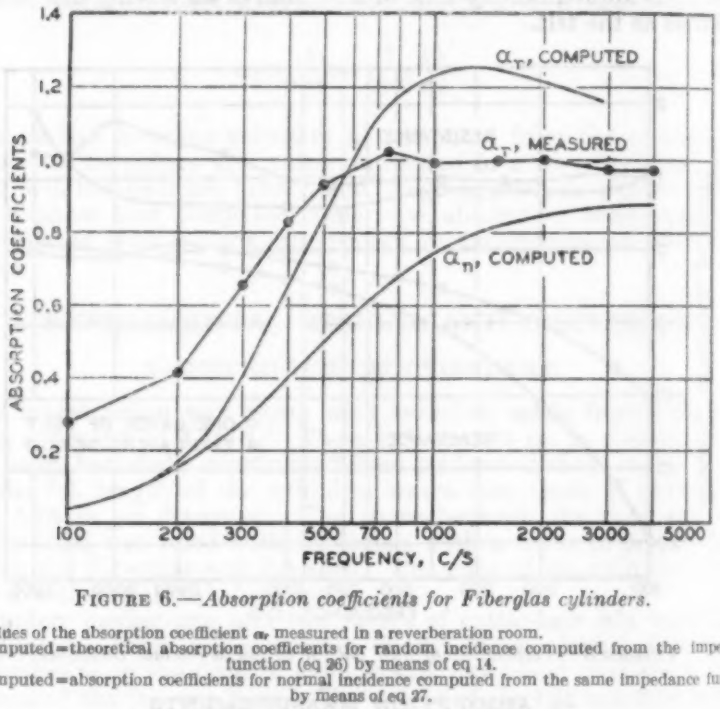

FIGURE 6.—*Absorption coefficients for Fiberglas cylinders.*

●=values of the absorption coefficient α_r measured in a reverberation room.
α_r, computed=theoretical absorption coefficients for random incidence computed from the impedance function (eq 26) by means of eq 14.
α_n, computed=absorption coefficients for normal incidence computed from the same impedance function by means of eq 27.

Figures 7 and 8 show curves for the cylinders having one and two layers of hair felt, respectively. The theoretical values of α_r were computed from the measured impedances given in figure 5 by means of eq 14. Also, the measured absorption coefficients for both one and two layers of hair felt laid flat on the floor of the reverberation room are plotted in figures 7 and 8, respectively. Comparison of the measured values for the flat layers with the corresponding measured cylinder coefficients shows that a given area of felt has considerably greater absorption, at higher frequencies, when wrapped on a cylinder than when applied to a flat surface.

Both the theoretical and measured reverberation-room coefficients

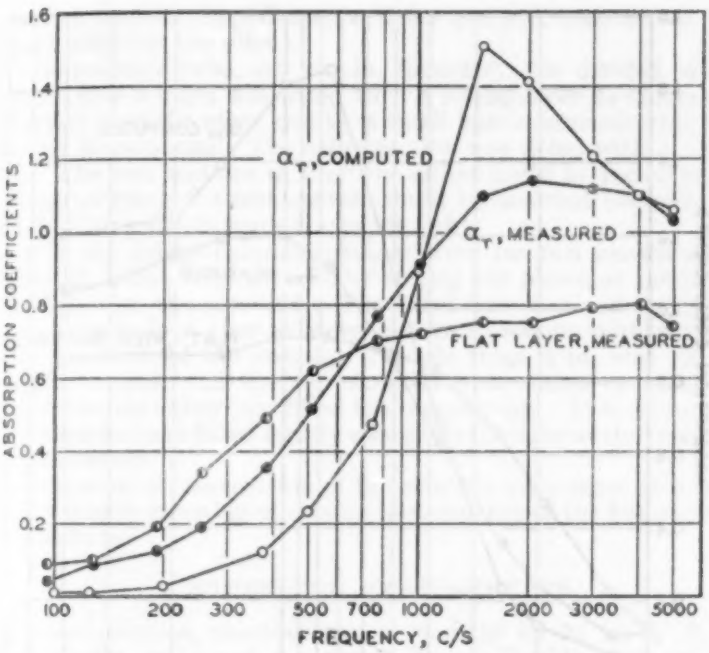

FIGURE 7.—*Absorption coefficients for cylinders with one layer of hair felt.*

○=theoretical values of the absorption coefficient α_r computed from inpedances given in figure 5 by means of eq 14.

●=values of α_r measured in a reverberation room.

◐=absorption coefficients for a flat single layer of hair felt measured in a reverberation room.

α_r show again that absorbent cylinders can have absorption coefficients greater than unity at frequencies corresponding to values of ka near unity. However, the maximum theoretical coefficients are somewhat greater than the maximum measured values. The exact location of the frequency of maximum absorption depends, of course, on the way in which the normal impedance varies with frequency, as well as on the value of ka. Consequently, the measured frequencies of maximum absorption for the two types of cylinders correspond to different values of ka. For the cylinders with one layer of felt, figure 7 shows the value of ka to be 2.7. For the cylinders with two layers, figure 8 shows the value to be 2.1.

Although there is general agreement between the theoretical and measured curves in each case, the differences at some frequencies are too great to be ascribed to experimental uncertainty. The theoretical coefficients are too low at low frequencies, too high at frequencies near $ka=1$, and are in fairly good agreement with the measured coefficients at high frequencies.

The differences between the theoretical and measured values of α_r might be explained qualitatively as follows: (1) The original assumption that the normal impedance completely describes the state of vibration of the air at the surface of the cylinder might be too simple. Sound waves might be propagated through the felt tangentially to the surface. If this should occur, the boundary conditions to be used in

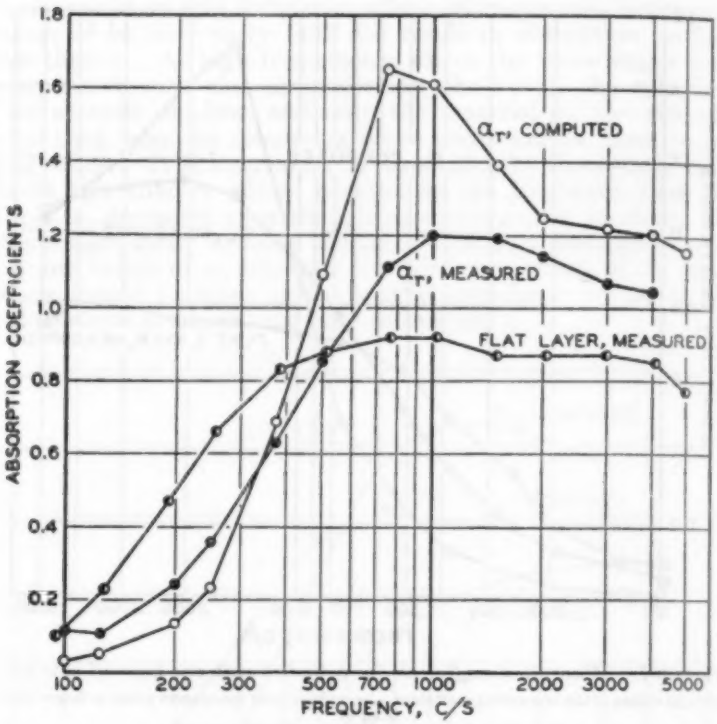

FIGURE 8.—*Absorption coefficients for cylinders with two layers of hair felt.*

○=theoretical values of the absorption coefficient α_T computed from impedances given in figure 5 by means of eq 14.
●=values of α_T measured in a reverberation room.
◐=absorption coefficients for a flat double layer of hair felt measured in a reverberation room.

solving the wave equation would be different. (2) The assumption that the absorption of a plane wave having an angle of incidence ϑ (see fig. 3) is directly proportional to cos ϑ is only an approximation, as has been mentioned before. (3) The statistical assumption that the wave motion is completely random in the particular reverberation room in which the measurements were made is a close approximation at higher frequencies, but might be incorrect at low frequencies.

Of the three conjectures, (1) and (2) will most likely explain the discrepancies observed. It is difficult to put these on a quantitative basis. The low theoretical values of α_T at low frequencies might be explained by (2), and the high theoretical values near $ka=1$ might be due to the tangential propagation of sound described in (1).

VI. EXPERIMENTAL PROCEDURE

1. IMPEDANCE MEASUREMENTS

The method used for measurement of the acoustic impedance of the felt was an adaptation of a method suggested by Flanders [4]. In the modified method, the unknown impedance was measured in terms of

two known acoustic impedances and the complex ratio of one bridge balance reading to two others.

The impedance tube, 3.2 cm in diameter, was divided into two sections. One section was fitted with a loudspeaker at one end, and was tapped near the other end by a small hole communicating with a condenser microphone. The other section was fitted with a movable piston. The two sections of the tube either could be joined together or a ring carrying the test sample could be inserted between them. A closely fitting sleeve made the joints tight.

Two of the bridge-balance readings were for two known acoustic impedances, which were secured by setting the piston at the junction and at $\lambda/8$ from the junction. The third was obtained by inserting the felt sample in a ring between the two sections with the piston against the back of the sample. Sample rings ⅞ in. and 1¾ in. in length were used, and the felt samples were either compressed or fluffed out so that they just filled the sample ring. It was found that the felt sample disks fitted tightly enough in the tube so that cementing was unnecessary.

Simultaneous measurements of the acoustic impedance of a tube of arbitrary length served as checks on the accuracy of the felt impedance determinations.

2. ABSORPTION MEASUREMENTS

The reverberation chamber was a room 30 by 25 by 20 ft, with smooth plaster walls and a concrete floor. Double-brick wall construction prevented extraneous noise.

Rotating vanes, 8 by 16 ft over all, aided in the attainment of random wave conditions. Furthermore, the source of sound was modulated in frequency, or "warbled", through ± 10 percent of the nominal signal frequency. The loudspeakers were mounted on the vanes.

The sound was picked up by four stationary microphones. After preamplification, the outputs from the four microphones were fed into a commutating device that sampled the outputs successively 12 times a second. After further amplification, the output was filtered by means of a band pass filter.

The decay of the residual sound in the reverberation chamber was recorded on an automatic logarithmic power-level recorder working over a range of 50 decibels. Decay curves for the empty chamber were obtained before and after the absorbent materials were placed in the chamber in order to minimize any effects due to temperature and humidity changes. Care was taken to keep the amount of absorbent material in the chamber well below the quantity required to produce nonlogarithmic decays. In all, 10 decay curves for both the empty chamber and the chamber with material were recorded at each frequency. The final total absorption A was computed from the formula

$$A=\frac{4V}{c}\left(\log_e 10^5\right)\left(\frac{1}{T_M}-\frac{1}{T_E}\right), \tag{28}$$

where T_M and T_E are the 50-decibel decay times in the room containing the absorbent material and in the empty room, respectively.

The individual Fiberglas cylinders were joined together to form two long cylinders, each 32.3 ft long, and were supported on trestles with the centers of the cylinders 34 in. above the floor. The perpendicular distance between the two long cylinders was 12.1 ft.

Both the single-layer and double-layer felt-covered cylinders were arranged in two different ways. In one arrangement, three cylinders 30.4 ft long were assembled from the cylinder sections placed end to end. The perpendicular distance between the centers of the long cylinders was 15.7 ft. In the other arrangement, five cylinders 19.9 ft long were assembled from two sections each and were spaced 5 ft on centers. For the single-layer-covered cylinders, the centers were 50 in., and for the double layer, 54 in. above the floor of the reverberation chamber. All free ends of the cylinders were stuffed with hair felt to prevent any possible standing waves at the lower frequencies. All free ends were also capped with sheet iron.

The absorption coefficients of both one and two layers of felt laid flat on the floor of the reverberation room were determined on approximately square samples, each having an area of about 80 ft.^{2} The coefficients were extrapolated to what they would be for an infinite area by means of corrections empirically determined by Chrisler [5].

VII. ACCURACY OF MEASUREMENTS

The estimate of the accuracy of the impedance measurements of the hair felt was based on (1) the agreement between the computed and the experimental values of the impedance of a tube l cm long measured simultaneously with the felt samples, and (2) the precision as given by repeated measurements. It was found that the impedance of the tube computed from

$$\frac{Z}{\rho c} = -i \cot (kl) \tag{29}$$

agreed within 3 percent with the experimental value, except for those frequencies at which the impedance approached zero. In agreement with Flanders [4], it was also found that the resistive component was very small, provided the tube length did not approach $(n\lambda/2)$ $(n=1, 2, 3 \ldots)$. The resistive component, for a tube of length $l=6$ cm, fluctuated between negative and positive values, averaging about 2 percent of the reactive component. The results of repeated measurements on the 6-cm tube, and also on the felt, agreed within 4 percent through about 2,000 c/s. Above this frequency, the variation in repeated measurements on the tube averaged about 7 percent. The final uncertainty ascribed to the impedance measurements on the felt is 5 percent.

In evaluating the uncertainty in the measurement of absorption coefficients on the assumption that Sabine's formula holds for the reverberation chamber, all that needs to be considered is the repeatability of the decay times and the agreement by different observers in reading the decay curves. All other factors in the reverberation formula are known with relatively high accuracy. Due to the irregularities in the decay curves at the lowest frequencies, the uncertainty in the decay times may be as high as 6 percent. The uncertainty decreases rapidly with increasing frequency until, beginning at about

250 c/s, it is about 2 percent. As the absorption coefficients are directly proportional to the difference between the reciprocals of two decay times, the estimated final uncertainty is about 3 percent for the greater part of the frequency range.

Absorption measurements were made on cylinders of finite length, whereas the theoretical coefficients were deduced for infinitely long cylinders. As at almost all frequencies the absorption coefficients for the cylinders 19.9 ft long and 30.4 ft long mentioned above differed by less than the experimental uncertainty, it is believed that the end effects are negligible. The absorption coefficients given in figures 7 and 8 are the averages for the cylinders of different lengths.

VIII. TECHNIC OF CALCULATION

Bessel functions of high order and their derivatives were needed to compute α_r (eq 14). It was decided that the British Association Mathematical Tables [6] would yield accurate results more quickly than would any other available tables of Bessel functions. First, values of ka (which are the arguments of the Bessel functions) were computed to three decimal places from the measured circumferences of the cylinders and the frequencies used in making the normal impedance measurements. The values of ka used in the calculations ranged from about 0.13 to about 8.7. The Bessel functions of high order were computed from the British Association Tables for J_0, J_1, Y_0, and Y_1 by means of well-known recurrence formulas.

Enough terms in the infinite series of eq 14 were used so that the estimated sum of the remainder terms amounted to less than 0.1 percent of the whole sum. It is believed that the final computed values of the absorption coefficients α_r have errors (arising from the sequence of calculations) of less than 0.01.

IX. SUMMARY

A wave theory has been applied to the absorption of sound by an absorbent circular cylinder of infinite length. An exact expression, including the effects of diffraction, has been obtained for the absorption coefficient of a cylinder on which is incident a plane wave of sound traveling in a direction perpendicular to the axis of the cylinder. The derivation of the expression for the absorption coefficient was based on the assumption that the ratio of sound pressure at a point on the cylinder surface to the normal component of particle velocity was equal to the normal acoustic impedance of the surface. Theoretical coefficients were computed for Fiberglas cylinders by using assumed impedances and were computed for cylinders of hair felt by using impedances that were measured directly.

The theoretical coefficients were compared with experimental values obtained for cylinders placed in a reverberation room. In order to effect the comparison, it was necessary to develop the statistics for the absorption by a cylinder located in a random wave field. These statistics were shown to be different from the usual statistics that apply to the absorption by a flat patch on a wall of a reverberation room.

The theory predicts, and measurements confirm, that absorbent cylinders can have coefficients greater than unity. The agreement between the theoretical and experimental coefficients is fairly good, and is better than that usually found for flat patches of absorbent material placed in a reverberation room. The discrepancies between theoretical and experimental coefficients appear to be due either to wave propagation through the absorbent material in directions tangential to the surface, to absorption at oblique incidence that is not directly proportional to the cosine of the angle between the direction of propagation of the incident sound and a plane normal to the cylinder axis, or to a combination of these two effects.

The statistics for the absorption by a sphere located in a random wave field were developed. Comparison of theoretical and experimental absorption coefficients for spheres would be of great interest. There would be no uncertainty for spheres about the absorption at oblique incidence as there is for cylinders and flat patches of absorbent material.

X. REFERENCES

[1] G. Jäger, Sitzungsber. Akad. Wiss. Wien IIa **120,** 613 (1911).
[2] E. Buckingham, Sci. Pap. BS **20,** 193 (1925) S506.
[3] L. L. Beranek, J. Acous. Soc. Am. **13,** 14 (1940).
[4] P. B. Flanders, Bell System Tech. J. **11,** 402 (1932) Republished in J. Acous. Soc. Am. **4,** July supp. (1932).
[5] V. L. Chrisler, J. Research NBS **13,** 169 (1934) RP700.
[6] British Association Mathematical Tables, vol. VI, Bessel functions (University Press, Cambridge, 1937).

WASHINGTON, December 17, 1945.

U. S. DEPARTMENT OF COMMERCE NATIONAL BUREAU OF STANDARDS

RESEARCH PAPER RP1710

Part of Journal of Research of the National Bureau of Standards, Volume 36, April 1946

DYNAMIC TENSILE TESTS OF PARACHUTE WEBBING

By Ambrose H. Stang, Martin Greenspan, and Sanford B. Newman

ABSTRACT

Dynamic-load–stretch and stretch-energy data were obtained for two types of nylon and one type of cotton parachute webbing. These data were compared with similar data obtained from static tensile tests of the materials. The dynamic and static breaking strengths of the webbing were also obtained.

The nylon specimens showed a reduced strength, stretch, and capacity for energy absorption under dynamic loading as compared with static loading. The cotton specimens showed under dynamic loading about the same strength, reduced stretch, and increased energy absorption. The energy absorbed by the broken nylon specimens was more than three times that of the broken cotton specimens.

CONTENTS

	Page
I. Introduction	411
II. Specimens	412
III. Description of tests	412
1. General	412
2. Maximum stretch, over-all set, and free-length set	412
3. Load	412
4. Load-stretch relation	413
5. Energy	414
6. Static tests	414
IV. Results and discussion	414
1. Load-stretch relations	414
2. Stretch-work relations	415
3. Maximum values	417
V. References	419

I. INTRODUCTION

At the request of the Bureau of Aeronautics, Navy Department, the National Bureau of Standards undertook comparative tests on various types of parachute webbing. The load-stretch relationships and other mechanical properties of three types of webbing under dynamic tensile loading were investigated. The loads were to be applied by means of a 200-lb mass falling through a height sufficient to produce in the webbing a tensile force of 4,000 lb (an acceleration of the falling mass of 20 g).

High-speed tensile-test data for textile materials are comparatively rare; hence the results of these tests are of some general interest, even though the test specimens were specialized and the ranges of variables investigated were narrow. The method of obtaining the dynamic-

load–stretch relationship is similar in principle to that used on metals by Clark and Dătwyler [1].[1]

II. SPECIMENS

The three types of 1¾-in.-wide parachute webbing tested were identified as rib-weave nylon, herringbone-weave nylon, and type *X* herringbone-weave cotton. The types of webbing are shown in figure 1. Each specimen consisted of a length of webbing held by a heavy D-ring (with cross bar) at the top and by two similar D-rings at the bottom, as shown in figure 2. The clear inside distance between D-rings was 36.0 in. in all cases. The test results given in this report apply to the complete specimen, including the D-rings.

III. DESCRIPTION OF TESTS

1. GENERAL

The test setup is shown in figure 2. The specimen was hung from a 1⅝-in.-diameter steel bar held in the fixed head of a testing machine. (The testing machine was used only as a support and for calibration purposes.) A steel weight pan was suspended from the lower D-rings by means of a connecting link. The combined mass of the weight pan and link was 13.7 lb.

The falling weight, which had a mass of 198.5 lb, consisted of a steel cylindrical annulus with a hole large enough to clear the rod, the specimen, and the connections. The weight was hung from the movable head of the testing machine by light sash cord. The movable head was positioned to give the desired height of drop, and the weight was released by cutting the cord.

2. MAXIMUM STRETCH, OVER-ALL SET, AND FREE-LENGTH SET

The maximum stretch of the specimen was obtained from the depression of the column of modeling clay directly under the weight pan. The length of the specimen under the load of the weight pan was considered the initial length (zero stretch).

The clear inside distance between D-rings was measured before (36.0 in.) and after the drop with the weight pan in place.

Before the drop, a 20-in. gage line was marked on the webbing with pins, and the gage line was measured after the drop with the weight pan in place.

3. LOAD

The connection between the upper end of the specimen and the lower end of the 1⅝-in. rod consisted of a connecting link and a ¾-in. eyebolt arranged as a dynamometer. Several inches of the shank of the eyebolt had been reduced to ⅝-in. diameter and four *SR–4* wire strain gages, type A7, were cemented to the reduced surface. Two of the gages were parallel to the axis of the shank and were connected in series, the other two, also in series, were at right angles to the axis.

[1] Figures in brackets indicate the literature references at the end of this paper.

The two pairs of gages were connected as adjacent arms in an a-c Wheatstone bridge. The output of this (unbalanced) bridge was proportional to the tensile load on the eyebolt.

The voltage on the bridge was 10 volts, 1,000 cycles per second, produced by an electronic oscillator. The output of the bridge was amplified and the demodulated signal made available for recording on an oscillograph recorder that produced a photographic record of load versus time.

A load of 4,000 lb on the dynamometer produced a deflection on the record of about 0.65 in. Calibrations of the dynamometer by means of the testing machine were made several times daily while the tests were in progress. The time scale on the record was marked by lines about ¼ in. apart, corresponding to time intervals of 0.01 sec. The duration of test from beginning of impact to maximum load was about 0.05 to 0.06 sec for the nylon and 0.03 to 0.04 sec for the cotton specimens.

The natural frequency of the dynamometer was, of course, very high compared to that of the specimen, and the natural frequency of the galvanometer coil was 430 cycles per second. Typical oscillograms are shown in figure 3.

4. LOAD-STRETCH RELATION

The forces acting on the combined mass, $M+m$, of the falling weight and weight pan are the weight, $(M+m)g$, acting downward (positive); the tension, $F=F(t)$, given on the oscillogram, and the initial load due to the weight pan, mg, acting upward. Hence the differential equation for the stretch, $s=s(t)$, is, by Newton's law,

$$(M+m)g-F-mg=(M+m)\frac{d^2s}{dt^2},$$

or

$$\frac{d^2s}{dt^2}=\frac{Mg}{M+m}-\frac{F}{M+m}. \tag{1}$$

Here F is in absolute units (poundals). Since F is given as $F(t)$ on the oscillogram, eq 1 may be integrated numerically for $s(t)$. Elimination of t between $F=F(t)$ and $s=s(t)$ gives the load-stretch relationship.

If t is taken as zero at the beginning of impact, then the initial condition for s is $s=0$ when $t=0$. The velocity of the weight just before impact is $\sqrt{2gh}$, where h is the height of drop. Upon impact (assumed plastic), the common velocity of the weight and pan is reduced to

$$v_0=\frac{M}{M+m}\sqrt{2gh} \tag{2}$$

in accordance with the principle of conservation of momentum. This is the initial condition on the velocity required for the integration.

The maximum stretch computed by this method may be compared with that given by the clay-column measurement.

5. ENERGY

The work done on the specimen, corresponding to various stretches, was obtained by evaluating numerically the integral $\int_0^s F ds$. The maximum work, $\int_0^{s_m} F ds$, where s_m is the maximum stretch, was compared with the "input energy," E. In cases where no failure occurred the input energy was equal to the sum of the kinetic energy at the instant of impact and the potential energy lost during stretching.

$$E = \frac{(M+m)v_0^2}{2} + (M+m)gs_m$$

$$= \frac{M}{M+m} Mgh + (M+m)gs_m. \quad (3)$$

6. STATIC TESTS

For comparison, one specimen of each type of webbing, in all respects identical with the dynamic-test specimens, was tested at slow speed (4 in./min) in a horizontal testing machine. Load-stretch data to failure were obtained, and the stretch-energy relations were computed as for the dynamic tests.

IV. RESULTS AND DISCUSSION

1. LOAD-STRETCH RELATIONS

The results for the individual dynamic tests are given in tables 1, 2, and 3. Because the load corresponding to a given stretch showed no consistent variation with height of drop, the results were averaged for each type of webbing and compared with the results of the static tests. The load and stretch are reckoned as zero when the tension in the specimen is equal to the weight of the weight pan, about 14 lb.

TABLE 1.—*Load-stretch data for rib-weave nylon*

Stretch	Specimen number						Average dynamic	Static
	1	2	3	4	5	6		
	Load							
in.	*lb*	*lb*	*lb*	*lb*	*lb*	*lb*	*lb*	*lb*
0	0	0	0	0	0	0	0	0
1	220	160	240	130	220	200	190	80
2	440	350	460	280	430	410	390	220
3	660	590	680	470	700	610	620	420
4	880	810	910	660	1,020	810	850	690
5	1,100	1,080	1,150	850	1,340	1,010	1,090	800
6	1,360	1,390	1,400	1,070	1,700	1,240	1,360	1,080
7	1,670	1,770	1,680	1,370	2,030	1,530	1,670	1,390
8	2,000	2,130	2,000	1,740	2,380	1,860	2,020	1,750
9	2,380	2,520	2,370	2,170	2,780	2,310	2,420	2,190
10	2,850	2,880	2,770	2,630	3,210	2,750	2,850	2,690
11	3,340	3,250	3,220	3,020	3,740	3,190	3,290	3,310
12	3,680	3,640	3,610	3,390	4,200	3,620	3,700	4,000
13	-----	-----	3,940	3,940	-----	3,960	-------	4,800
14	-----	-----	-----	-----	-----	-----	-------	5,750

TABLE 2.—*Load-stretch data for herringbone-weave nylon*

Stretch	Specimen number										Average dynamic	Static
	7	8	9	10	11	12	13	14	15	16		
	Load											
in.	*lb*	*lb*	*lb*	*lb*	*lb*	*lb*	*lb*	*lb*	*lb*	*lb*	*lb*	*lb*
0	0	0	0	0	0	0	0	0	0	0	0	0
1	250	240	200	460	290	210	260	440	250	320	290	80
2	500	500	400	840	540	510	540	660	520	600	560	270
3	750	770	590	1,110	750	780	810	880	790	840	810	480
4	1,010	1,050	800	1,260	1,020	1,060	1,110	1,130	1,130	1,100	1,070	740
5	1,290	1,370	1,100	1,570	1,350	1,380	1,420	1,390	1,480	1,390	1,370	1,040
6	1,610	1,720	1,440	1,910	1,710	1,730	1,770	1,700	1,900	1,730	1,720	1,370
7	2,000	2,120	1,800	2,300	2,130	2,080	2,170	2,100	2,360	2,150	2,120	1,760
8	2,370	2,590	2,240	2,640	2,560	2,500	2,630	2,580	2,830	2,680	2,560	2,230
9	2,790	3,100	2,710	3,150	3,050	3,100	3,110	3,100	3,300	3,220	3,060	2,770
10	3,340	3,620	3,230	3,980	3,520	3,720	3,610	3,650	3,750	3,710	3,610	3,440
11	3,880	---	3,770	---	3,800	4,120	3,980	3,890	---	---	---	4,210
12	---	---	4,250	---	---	---	---	---	---	---	---	5,080

TABLE 3.—*Load-stretch data for herringbone-weave cotton*

Stretch	Specimen number						Average dynamic	Static
	17	18	19	20	21	22		
	Load							
in.	*lb*	*lb*	*lb*	*lb*	*lb*	*lb*	*lb*	*lb*
0.0	0	0	0	0	0	0	0	0
.5	60	170	40	160	80	160	110	30
1.0	200	360	180	500	220	440	320	60
1.5	400	590	460	1,060	460	860	640	170
2.0	660	870	1,040	1,810	940	1,580	1,150	370
2.5	1,010	1,370	1,600	2,800	1,710	2,460	1,820	770
3.0	1,670	2,280	2,360	3,830	2,700	3,420	2,710	1,350
3.5	2,890	3,260	3,250	-----	3,570	4,030	3,400	2,190
4.0	-----	-----	-----	-----	-----	-----	-----	3,290

It will be seen from these tables that the dynamic-load values are greater than the static-load values for equal stretches, except for the rib-weave nylon webbing for stretches of 11 and 12 inches. The difference between the dynamic- and static-load stretch values is greater for the cotton webbing than for the nylon webbings.

2. STRETCH-WORK RELATIONS

The stretch-work results are given in tables 4, 5, and 6, which are arranged in the same way as tables 1, 2, and 3. For equal stretches, the average dynamic work values are greater than the static work values.

TABLE 4.—*Stretch-work data for rib-weave nylon*

Stretch	Specimen number						Average dynamic	Static
	1	2	3	4	5	6		
	Work							
in.	*ft-lb*	*ft-lb*	*ft-lb*	*ft-lb*	*ft-lb*	*ft-lb*	*ft-lb*	*ft-lb*
0	0	0	0	0	0	0	0	0
1	9	5	11	5	5	8	7	4
2	37	35	40	22	35	34	30	20
3	82	66	88	53	82	76	70	50
4	147	122	155	100	154	134	130	90
5	229	203	241	163	250	210	220	150
6	332	312	346	243	377	304	320	230
7	458	443	474	345	530	418	440	340
8	607	600	627	474	720	560	600	470
9	789	800	809	636	930	734	780	630
10	1,010	1,020	1,020	836	1,180	945	1,000	840
11	1,270	1,280	1,270	1,070	1,470	1,200	1,260	1,080
12	1,560	1,560	1,560	1,340	1,800	1,480	1,550	1,400
13	-----	-----	1,870	1,640	-----	1,790	-------	1,760
14	-----	-----	-----	-----	-----	-----	-------	2,190

TABLE 5.—*Stretch-work data for herringbone-weave nylon*

Stretch	Specimen number										Average dynamic	Static
	7	8	9	10	11	12	13	14	15	16		
	Work											
in.	*ft-lb*	*ft-lb*	*ft-lb*	*ft-lb*	*ft-lb*	*ft-lb*	*ft-lb*	*ft-lb*	*ft-lb*	*ft-lb*	*ft-lb*	*ft-lb*
0	0	0	0	0	0	0	0	0	0	0	0	0
1	11	10	9	20	13	10	11	22	13	14	10	4
2	42	40	35	75	48	36	44	67	48	53	50	20
3	93	94	77	156	102	88	100	132	99	113	110	50
4	166	169	135	253	175	167	180	215	175	194	180	100
5	261	270	215	370	273	268	285	319	283	298	280	180
6	382	399	320	516	401	400	417	448	428	428	410	280
7	532	559	455	691	562	560	580	606	607	590	570	410
8	714	756	624	897	756	750	780	801	812	790	770	580
9	929	989	831	1,130	989	980	1,020	1,040	1,070	1,040	1,000	780
10	1,180	1,270	1,080	1,430	1,260	1,270	1,300	1,320	1,360	1,330	1,280	1,040
11	1,480	-----	1,370	-----	-----	-----	1,620	1,630	-----	-----	-----	1,360
12	-----	-----	1,710	-----	-----	-----	-----	-----	-----	-----	-----	1,750

TABLE 6.—*Stretch-work data for herringbone-weave cotton*

Stretch	Specimen number						Average dynamic	Static
	17	18	19	20	21	22		
	Work							
in.	*ft-lb*	*ft-lb*	*ft-lb*	*ft-lb*	*ft-lb*	*ft-lb*	*ft-lb*	*ft-lb*
0.0	0	0	0	0	0	0	0	0
.5	2	7	1	3	3	3	3	1
1.0	12	21	5	19	8	16	13	3
1.5	29	35	20	54	24	42	34	7
2.0	52	65	52	110	56	91	71	18
2.5	88	113	102	208	110	174	116	42
3.0	140	185	185	345	202	295	225	86
3.5	228	300	300	-----	336	455	324	160
4.0	-----	-----	-----	-----	-----	-----	-------	274

3. MAXIMUM VALUES

Table 7 gives the maximum load; the maximum stretch both measured (clay column) and computed (eq 1); the sets; the input energy (eq 3); and the maximum work (integration of load-stretch curve) for the dynamic-test specimens.

The maximum stretch computed by integration of eq 1 is consistently higher than the stretch measured by means of the clay column. This discrepancy is probably due to accumulation of systematic errors in the load-measuring equipment and gives an indication of the accuracy of the loads and stretches determined by the method described. However, the agreement between the input energy and the maximum work obtained by integration of the load-stretch relationship is excellent.

The set in the entire free length of the webbing is less than half the over-all set. This shows that slippage, as well as stretch, took place during the loading and emphasizes the fact that the specimen under test must be considered as the entire assembly, including the connections.

TABLE 7.—*Maximum values for specimens tested under dynamic loading*

Specimen number	Height of drop	Maximum load	Maximum stretch		Set		Input energy	Maximum work
			Measured	Computed	Over-all	20-in. free length		
	ft.	*lb.*	*in.*	*in.*	*in.*	*in.*	*ft-lbl*	*ft-lb*
RIB-WEAVE NYLON								
1	9.0	3,830	12.3	13.1	4.7	1.2	1,880	1,900
2	9.0	3,880	12.2	13.0	4.8	1.3	1,880	1,870
3	9.5	3,950	12.2	13.4	4.7	1.1	1,980	1,980
4	9.5	4,130	13.4	14.0	5.0	1.2	2,000	1,970
5	9.5	4,300	12.6	12.4	4.6	1.1	1,980	1,940
6[a]	10.0	4,050		13.5				1,960
HERRINGBONE-WEAVE NYLON								
7	8.0	3,650	10.4	11.8	3.9	1.1	1,670	1,720
8	8.5	4,000	10.5	11.5	4.1	1.1	1,760	1,730
9	8.5	4,250	10.6	12.2	4.2	1.2	1,760	1,760
10	8.5	4,400	11.0	10.9	4.4	1.1	1,770	1,760
11	8.5	3,800	10.6	11.5	3.9	1.2	1,760	1,740
12	8.5	4,180	11.1	11.5	3.9	1.0	1,770	1,750
13	9.0	4,110	11.3	11.8	4.0	1.1	1,870	1,890
14	9.0	3,910	10.6	12.0	4.4	1.2	1,850	1,930
15[a]	9.0	4,070		10.8				1,630
16[a]	9.5	3,940		10.6				1,560
HERRINGBONE-WEAVE COTTON								
17	1.5	3,110	3.4	3.9	2.5	0.6	340	350
18	1.75	3,270	3.2	3.8	2.2	.5	380	380
19	2.0	3,520	3.2	3.9	2.2	.5	440	440
20	2.0	3,880	3.1	3.3	2.1	.5	430	420
21[a]	2.25	4,000		3.9				480
22[a]	2.5	4,060		3.5				460

[a] Webbing broke at upper D-ring.

The results show a considerable variability in the properties of the specimens. It should be remembered, however, that the specimens consisted of a length of webbing with D-rings at both ends, initially

under a load of only 14 lb. Differences in the amount of slippage during test and variability in the properties of the webbing from specimen to specimen would tend to induce different results for similar specimens.

Table 8 gives the maximum load, stretch, and work for the dynamic-test specimens that failed and for the static-test specimens. The maximum stretch for the dynamic-test specimens was computed from eq 1.

TABLE 8.—*Maximum values for specimens that broke*

Specimen number	Height of drop	Maximum load	Maximum stretch	Maximum work
	ft.	*lb*	*in.*	*ft-lb*
RIB-WEAVE NYLON				
6	10.0	4,050	13.5	1,090
Static		5,770	14.1	2,220
HERRINGBONE-WEAVE NYLON				
15	9.0	4,060	10.8	1,650
16	9.5	3,940	10.6	1,580
Static		5,450	12.5	1,971
HERRINGBONE-WEAVE COTTON				
21	2.25	4,000	3.9	600
22	2.50	4,060	3.5	480
Static		4,090	4.4	380

All the failures occurred in the webbing at the connection to the single D-ring. The cross bar of the D-ring was deformed during the static tests but was undamaged by the dynamic tests.

The nylon specimens had a reduced strength, stretch, and capacity for energy absorption under dynamic loading as compared with static loading.

The cotton specimens had under dynamic loading about the same strength, reduced stretch, and increased energy absorption. This apparent anomaly is due to the fact that the difference between the dynamic- and static-load–stretch values were greater for the cotton webbing than for the nylon webbings.

From table 8 it is noted that the values of maximum load and maximum work for the nylon webbing specimens subjected to dynamic loading, and which were broken, were less than for the specimens subjected to static loading. This is contrary to the generally accepted idea that the strength of textile specimens increases as the rate of load application increases [2, 3]. The parts of the nylon specimens, after failure, were found to be fused and very warm at the fracture at the D-rings. It is probable that owing to the high rate of load application during the dynamic tests at the greatest height-of-drop values, heat was generated at such a rate that the temperature increased enough to cause a decrease in the strength of the nylon webbing. The values of maximum load and of maximum work given in table 7 for the nylon specimens which were broken are not as great as for other similar specimens also subjected to dynamic loading but not broken.

It is again probable that the temperature of the specimens not broken was less than for the broken specimens and consequently the strength and ability to absorb energy was greater for those not broken than for the specimens which were broken.

The breaking loads for the dynamic-test specimens were all very close to the 4,000-lb value that had originally been designated as the load to be attained. The strength of the herringbone-weave nylon specimen No. 16 was less than this value. It seems from these results that the strength of the nylon specimens, as determined by static tensile tests, cannot be safely used to predict the dynamic-load strengths. The energy absorbed by the broken nylon specimens was more than three times that of the broken cotton specimens.

V. REFERENCES

[1] D. S. Clark and G. Dätwyler, Stress-strain relations under tension impact loading, Proc. ASTM **38** II, 98 (1938).
[2] C. G. Lutts and D. Himmelfarb, The creep phenomenon in ropes and cords, Proc. ASTM **40,** 1251 (1940).
[3] Sanford B. Newman and Helen G. Wheeler, Impact strength of nylon and of sisal ropes, J. Research NBS **35,** 417 (1945) RP1679.

WASHINGTON, January 10, 1946.

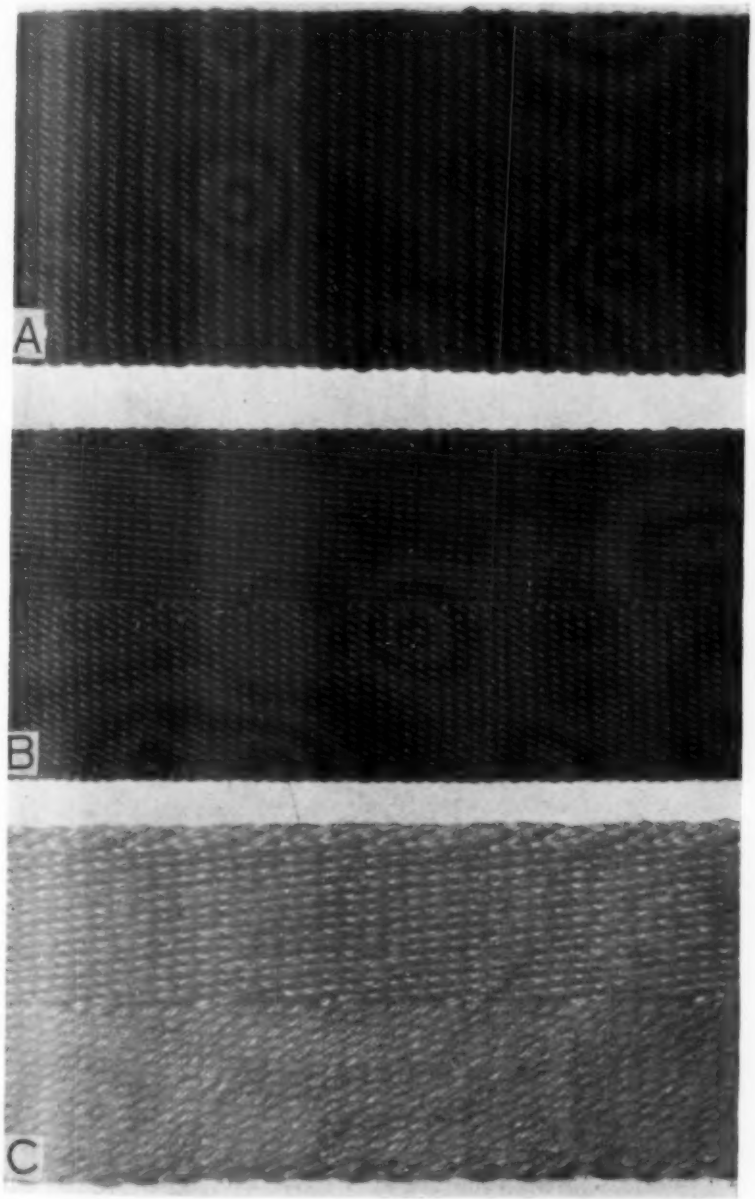

FIGURE 1.—*Samples of the types of webbing tested.*

A, rib-weave nylon; *B*, herringbone-weave nylon; *C*, type *X* herringbone-weave cotton.

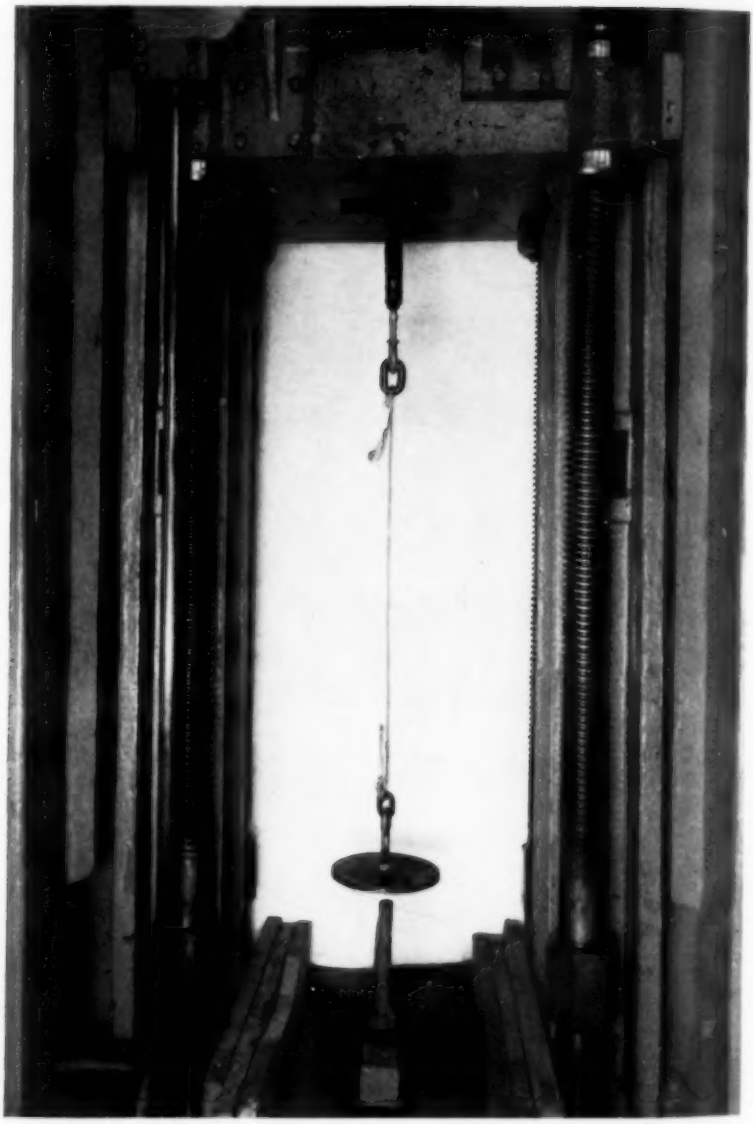

FIGURE 2.—*General view of test setup.*

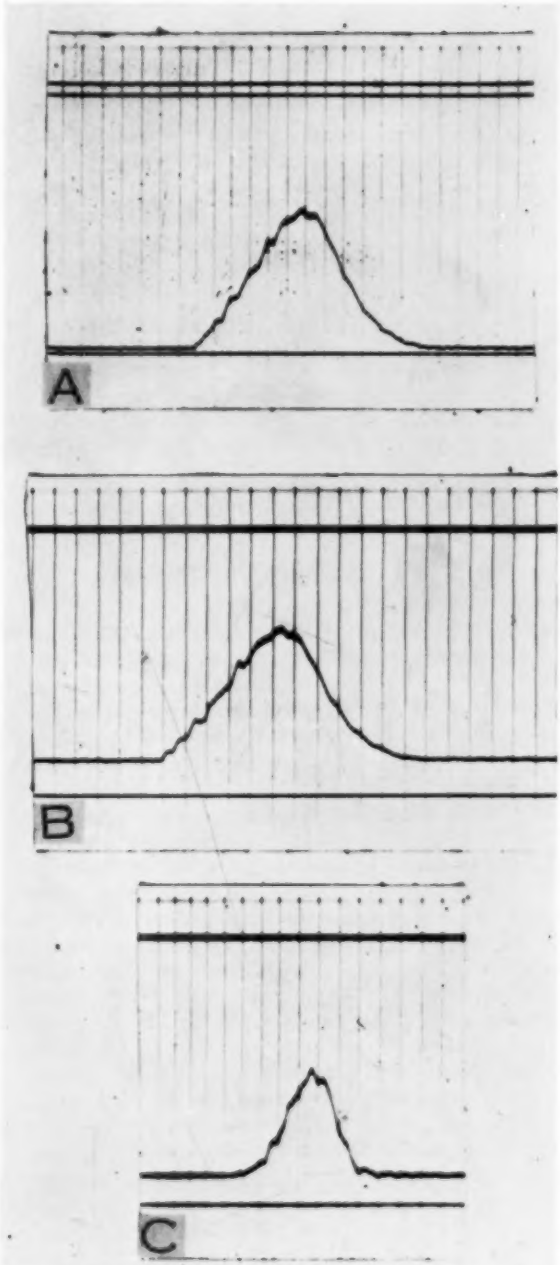

FIGURE 3.—*Typical oscillograms for rib-weave nylon, A, herringbone-weave nylon, B, and type X herringbone-weave cotton, C.*

U. S. DEPARTMENT OF COMMERCE NATIONAL BUREAU OF STANDARDS

RESEARCH PAPER RP1711

Part of Journal of Research of the National Bureau of Standards, Volume 36, April 1946

NOTE ON THE DENSITY AND HEAT OF COMBUSTION OF BENZOIC ACID

By R. S. Jessup

ABSTRACT

The results of various determinations of the density of benzoic acid are summarized. The three most recent values are in reasonably good agreement with each other, but are higher by about 4.5 percent than the value most commonly referred to in the literature. The difference of 4.5 percent in density affects the reduction of weight in air to mass by an amount corresponding to 0.004 percent in mass, and in heat of combustion per gram mass.

The value 26428.4 ±2.6 international joules per gram mass reported [1] [1] in 1942 for the heat of combustion of Bureau Standard Sample 39f of benzoic acid under the specified standard conditions of the bomb process was obtained from the experimental values of heat of combustion per gram weight in air, using the value 1.260 g/cm³ for the density of benzoic acid at 25° C in making the reduction to mass. This value was derived from the value 1.266 g/cm³ for the density at 15° C given in International Critical Tables [2], and the value 0.00053 per degree centigrade reported by E. R. Smith [3] for the coefficient of cubical expansion of benzoic acid in the range 15° to 30° C. The value of density given in ICT is apparently that reported by Lumsden [4] in 1905.

It has recently been noted that two other values have been obtained for the density of benzoic acid, namely, the value 1.322 g/cm³ at 20° C reported by Steinmetz [5] in 1913, and the value 1.3211 ± 0.0001 g/cm³ at 23.3° C reported by Hendricks and Jefferson [6] in 1933. Steinmetz gave no information regarding his method of measurement or the accuracy of his result. Hendricks and Jefferson made measurements on single crystals grown from melts, by suspending the crystals in an aqueous salt solution, varying the concentration until the crystals just floated when the system was subjected to a centrifugal force of about 400 times gravity, and determining the density of the solution by means of a picnometer. The results were corrected for the effect of compressibility of solution and crystals. The individual results were not reported, but the probable error of the mean value was given as ±0.0001 g/cm³.

[1] Numbers in brackets indicate the literature references at the end of this paper.

From the care with which the measurements of Hendricks a Jefferson were made, and from the agreement of their value wi that of Steinmetz, it would seem that the older value of Lumsden seriously in error. However, as no information was available r garding the reliability of the value reported by Steinmetz, and as was not absolutely certain that the difference between the values Lumsden and of Hendricks and Jefferson could be attributed entire to error in Lumsden's data, an independent determination of t density of benzoic acid seemed desirable. Since an accuracy of 1 the third decimal place is ample for the purpose of reducing weig in air to mass, it did not appear worth while to attempt to obta higher accuracy than this.

To obtain samples of benzoic acid on which density determin tions could be made, an attempt was made to grow single crysta from melts in the manner described by Hendricks and Jefferso The product obtained was examined microscopically by C. P. Sayl of the Chemistry Division of this Bureau, who reported that t samples were not single crystals, but were sufficiently compact a free from voids so that resasonably satisfactory density determin tions could be made on them.

The density determinations were made by Mildred W. Jones, of t Weights and Measures Division of this Bureau, by the method hydrostatic weighing in a saturated aqueous solution of benzoic ac The density of this solution was determined by Mrs. Jones by mea of a picnometer. Measurements on two samples of crystals prepar in separate experiments yielded the same value, namely, 1.316 g/c at 28° C.

The results of the various determinations of the density of benzo acid are given in table 1. The reduction to 25° C was made by usi for the coefficient of cubical expansion, γ, both the value 0.00040 r ported by Schwab and Wichers [7][2] and the value 0.00067 that was o tained by recalculating the data of Smith [2] using the value 1.319 g/c at 25° for the density of benzoic acid rather than the value 1.266 g/c at 15° C originally used by Smith. It will be seen from table 1 th although the two values of the coefficient of expansion differ conside ably, the difference has only a relatively small effect on the valu obtained for the density at 25° C. It will also be seen from table that the three most recent determinations are in reasonably sat factory agreement with each other, whereas the value of Lumsden lower by about 4.5 percent than the other three. It seems safe conclude that the value reported by Lumsden is seriously in erro Any of the other values would be satisfactory for use in reducin weight in air to mass, as the value obtained for mass by using 1.31 g/cm³ for the density would differ by less than 2 parts in a million fro that obtained with 1.3202 g/cm³. In view of the fact that voids in t samples of benzoic acid would result in low values of density, and b cause of the care with which the measurements of Hendricks a

[2] Schwab and Wichers calculated the density of solid benzoic acid at its melting point (by means of t Clausius-Clapeyron equation) from (1) their observed value of the pressure coefficient of the freez temperature, (2) a value derived from data reported by Timmermans and Burriel [8] for the density of t liquid at the freezing temperature, and (3) the value given in International Critical Tables for the heat fusion. The value 1.27 g/cm³ obtained in this way, and the value of density at 23.3° C reported Hendricks and Jefferson, were then used to calculate the mean coefficient of cubical expansion in t range from 23° to 122° C.

Jefferson were made and the high precision of their results, their value is probably the most reliable one. It is therefore recommended that the value 1.320 g/cm³ be used for the density of benzoic acid at 25° C for the purpose of reducing weight in air to mass.

TABLE 1.—*Values for the density of benzoic acid*

Observer	Density reported	Density at 25° C	
		γ=0.00040	γ=0.00067
	g/cm³	g/cm³	g/cm³
Lumsden (1905)	1.266 (15° C)	1.2610	1.2577
Steinmetz (1913)	1.322 (20° C)	1.3194	1.3176
Hendricks and Jefferson (1933)	1.3211 ±0.0001 (23.3° C)	1.3202	1.3196
Jones (this paper, 1945)	1.316 (28° C)	1.3176	1.3186

With 1.320 g/cm³ as the value for the density, the value for the heat of combustion of Standard Sample 39f of benzoic acid becomes 26429.4 ±2.6 international joules per gram mass when the sample is burned under the standard conditions [1] of the bomb process. It should perhaps be emphasized that when this standard sample of benzoic acid is used to calibrate a bomb calorimeter, no appreciable error would result from using the value originally reported [1] for the heat of combustion per gram mass of the sample, provided the value 1.260 g/cm³ is used for the density of benzoic acid at 25° C in reducing weight in air to mass.

---

[1] R. S. Jessup, J. Research NBS **29,** 247 (1942) RP1499.
[2] Int. Critical Tables **1,** 208 (1926).
[3] E. R. Smith, BS J. Research **7,** 903 (1931) RP382.
[4] J. S. Lumsden, J. Chem. Soc. **87,** 90 (1905).
[5] H. Steinmetz, Z. Krystallographie **53,** 463 (1913).
[6] S. B. Hendricks and M. E. Jefferson, J. Opt. Soc. Am. **23,** 299 (1933).
[7] F. W. Schwab and E. Wichers, J. Research NBS **34,** 333 (1945) RP1647.
[8] J. Timmermans and F. Burriel, Chimie & industrie, Special No. pp. 196–7 (March 1931).

WASHINGTON, December 17, 1945.

○